Document Title: Replication of Known Dental Characteristics in Porcine Skin: Emerging Technologies for the Imaging Specialist

Author(s): L. Thomas Johnson, Thomas W. Radmer, Dean Jeutter, Gary L. Stafford, Joseph Thulin, Thomas Wirtz, George Corliss, Kwang Woo Ahn, Alexis Visotky, Ronald L. Groffy

Document No.: 244568

Date Received: January 2014

Award Number: 2010-DN-BX-K176

REPLICATION OF KNOWN DENTAL CHARACTERISTICS IN PORCINE SKIN; EMERGING TECHNOLOGIES FOR THE IMAGING SPECIALIST

FINAL TECHNICAL REPORT

Award NIJ 2010-DN-BX-K176

L. Thomas Johnson[1]; Thomas W. Radmer[1]; Dean Jeutter[4]; Gary L. Stafford[1]; Joseph Thulin[2]; Thomas Wirtz[1]; George Corliss[4]; Kwang Woo Ahn[2]; Alexis Visotky[2]; Ronald L. Groffy[4].

1. Marquette University School of Dentistry; 2. Medical College of Wisconsin;

3.Marquette University College of Engineering;

4.Wisconsin Department of Justice, Crime Laboratory, (retired).

Replication of Known Dental Characteristics in Porcine Skin:

Emerging Technologies for the Imaging Specialist

NIJ 2010-DN-BX-K176

Award period October 1, 2010 – September 30, 2013

Johnson, LT[1]; Radmer, TW[1]; Jeutter, DC[3]; Corliss, GF[3]; Stafford, GL[1]; Wirtz, TS[1]; Groffy, RL[4]; Thulin, JD[2]; Ahn, KW[2]; Visotky, AD[2]

Abstract

This research project was proposed to study whether it is possible to replicate the patterns of human teeth (bite marks) in porcine skin, be able to scientifically analyze any of these patterns and correlate the pattern with a degree of probability to members of our established population data set.

The null hypothesis states: It is not possible to replicate bite mark patterns in porcine skin, nor can these bite mark patterns be scientifically correlated to a known population data set with any degree of probability.

Bite marks were produced on twenty-five pigs with a bite pattern replication device using 50 sets of models of blinded dentitions. The models were selected randomly from a previously quantified data set of 469. Prototyped dental models were mounted on a semi-automated mechanical device which records the model number, physical location on the pig where the force applied and the duration it was applied. Four patterns were created on each side of twenty-five anesthetized pigs in predetermined areas. These sites were tested previously in a pilot study; notably the hind quarter, abdomen, thorax and fore limb. Digital photographs of the patterned injuries (bite marks) were exposed following the guidelines of the Scientific Working Group on Imaging Technology (SWGIT) and the American Board of Forensic Odontology

Edited 10/11/13

(ABFO). Two hundred images of each dental arch were selected from the eight hundred photographs taken during the laboratory sessions and analyzed biometrically using a previously validated software program. Images were categorized as complete, partially complete or unusable, based on the presence, partial presence or absence of the six anterior teeth in each arch. Intersecting angles, the widths of the lateral and central incisors and the arch width measured on the scaled images of the unknown models. The images were analyzed independently by two investigators. Their measurements were then statistically compared to an established population data set of 469 males, ages 18 to 44 years. Statistical analysis was achieved using two models; Pearson's correlations and distance metric analysis. Pearson's correlation results based on width only, angle only and widths plus angles were reported by each investigator. Angles measured along with widths and compared to the known data set ranked each set of models from 1 to 469 with a ranking of one showing the lowest p values. Investigator #1 ranked 5 out of 143 images as number 1, 10 out of 143 in the top 1%, 34 out of 143 in the top 5% and 59 out of 143 in the top 10 %. Investigator #2 ranked 2 out of 156 as number 1, 13 out of156 in the top 1%, 36 out of156 in the top 5% and 54 out of 156 in the top 10%. The second statistical model using distance metric analysis had a sample count of 102 images with 3 out of 102 within 1% of the population, 16 out of 102 within 5% of the population and 23 out of 102 within 10% of the population when evaluating the results of the upper jaw only from investigator #1. The concept of using an incisal line is based on geometric principles of line segments and the angles they form when extended. The use of this concept will aid the crime laboratory imaging specialist and forensic odontologist in their analysis of bite marks (patterned injuries).

MeSH terms; forensic odontology, bite mark, dental characteristics, bite force, incisal line, quantification of dental characteristics, statistical analysis, load cell, FlexiForce sensor.

Edited 10/11/13

Table of Contents

Tables

Figures **Page**

Edited 10/11/13

Edited 10/11/13

Executive Summary

The National Academy of Science (NAS) 2009 report, *Strengthening Forensic Science in the United States: A Path Forward*, challenged the forensic science community to develop comprehensive reforms in research using scientific methodology, guidelines and standards for the analysis and reporting of an examiner's conclusions.

A research project was proposed to study whether it is possible to replicate the patterns of human teeth in skin (bite marks) and be able to scientifically analyze any of these patterns correlating them with a degree of probability to members of our established population data set.

The null hypothesis states; It is not possible to replicate bite mark patterns in porcine skin, nor can these bite mark patterns be scientifically correlated to a known population data set with any degree of probability.

A template was developed to be able to analyze and quantify the individual tooth characteristics in bite marks (patterned injuries) as they appear in a porcine skin. In order to establish a bite mark pattern, several considerations needed to be addressed.

These included selecting a suitable material to strong enough to duplicate natural tooth strengths, developing a mechanism to and accurately transfer a pattern of dental characteristics to porcine skin and developing a standardized method of mounting the dental models on a device which would produce a patterned injury (bite mark). It was also necessary to determine the force necessary to create a legible pattern in skin and calibrate each of the fifty replication device to deliver a standardized bite force for a specific time period. To be able to establish the probability that an image of a bite mark (patterned injury) on the pig could be correlated to a member (target) of the population data set with a level of probability, ranking the patterned injuries to the population data set was accomplished using both Pearson's correlations and a distance metric analysis model

Research Design

The selection of a material with natural tooth strengths included a trial using Castone™ dental models, cold cured methyl methacrylate dental resin and prototyping models using sintered steriolithography (SLS). The sintered form of prototyping by the 3M™ Corporation produced a model of the strength required for this research.

The use of a modified Irwin C-clamp to transfer patterns of dental characteristics to skin was previously reported. [17]. The incorporation of a load cell to calibrate each FlexiForce® transducer in each of the 50 pattern replication devices required to record the force applied had not previously been used. Initial trials of a prototype pattern replication device resulted in torqueing of upper models when force was applied. The use of ten parallel pins placed in the base of the upper dental models prevented this and ensured that all forces were directed to the incisal edges of the six anterior teeth and directly against the FlexiForce® transducer.

Force transducers, load cells and piezoelectric concepts were incorporated in the replicator device. Accurate measurement of the forces involved experimentation with materials that had limited hysteresis or fade during force loading. Ultimately a machined aluminum button attached to the piezoelectric sensor (FFT) provided for the most sustainable of compressive forces when applied for any interval of time.

The literature provides for a wide range of pounds force calibration in the incisor region from 20 to 122 PSI. These forces are influenced by numerous factors including pain, gender, age, musculature and the individuals existing occlusion. This study's determination of bite force necessary to create a patterned injury was based on a sampling of individuals between the ages of 22 and 32 showing a range of 25 to131.1 pounds force consistent with previous reports.

Calibration of each of the force sensors in the 50 replication devices by bench testing was accomplished prior to each animal laboratory session. A means of recording and sustaining the bite force for a 15 second time interval was required. This was accomplished with a complete Phidgets data acquisition system which consisted of a voltage divider, a precision voltage reference source, an Analog to Digital Converter board (ADC), USB interface and a laptop computer. Using a modification of a similar apparatus used in an earlier study the models were mounted on a modified Irwin™ welder's vise grip. By incorporating a force sensor, (FlexiForce® 100 lb. sensor), the Phidgets® device was bridged to a notebook computer running Lab View® software creating an auto-recording pattern replication device. This device allowed the replication of patterned injuries to be repeatable, consistent and measurable. The calibration procedure involved connecting the embedded FlexiForce® Transducer (FFT) to the Phidgets® data acquisition system and verifying its operation on the connected laptop computer running the custom software application, Lab View®. The load cell was placed in the replication apparatus, arranged mechanically in series with the embedded FFT sensor such that both transducers experienced the same biting force. Force was applied at 25, 50 and 100 pounds-force increments then removed at 50, 25 and 0 pounds force increments. Corresponding data from the FFT and the load cell were taken at each force increment and stored in a time and date stamped computer file for each of the 50 models and 50 corresponding pig locations.

Animal Laboratory Sessions

Animal research sessions were conducted in accordance with the standards of the *Guide for the Care and Use of Laboratory Animals* (8^{th} edition, National Academies of Sciences, 2011) and were approved by the Medical College of Wisconsin, Institutional Animal Care and Use Committee (IACUC).

Mixed-breed young pigs, weighing 30-40 kg were obtained from a commercial breeder and acclimated in the large animal laboratory research facility for a period of at least 2 days before the laboratory procedures were performed. Anesthesia was induced with a combination of tiletamine/zolazapam (Telezol®, 4.4 mg/kg) and xylazine (2.2 mg. /kg) administered intramuscularly. Following induction, an endotracheal tube was placed and hair from the anatomical sites of interest removed using a commercial hair clipper, razor, and/or depilatory cream. To conserve body temperature, animals were placed on heated pads on the surgical tables and covered with towels and a PolarSheild® Emergency Survival blanket (RothCo3015 Veterans Memorial Highway, Ronkonkoma, New York 11779-0512). The pigs' body temperatures were maintained between 36.2 and 39.3 degrees C and monitored by participating veterinary technicians. Using a rectal thermometer, the mean procedural temperature recorded was 38.1C (36.2C – 39.3C). The mean low 36.2C (33.9C – 37.0C) and the mean loss was 1.8C (0.2C – 4.3C). Following animal preparation, a surgical plane of anesthesia was maintained using isoflurane administered through the endotracheal tube using a precision vaporizer and compressed oxygen. Basal anesthesia was augmented as needed in some animals with pentobarbital administered intravenously to effect stage III general anesthesia.

The four designated sites to receive the patterned injury were the lateral aspects of the upper hind limb/thigh, abdomen/flank, thorax, and shoulder/upper forelimb of the animals. These were designated as site A, B, C and D referenced on the ABFO #2 scale label in the photographic image.

Photography

The injuries were digitally photographed at 1:1 scale (life size) by an forensic photographer 15 minutes after their creation, using a Cannon™ EOS 5d Mark II, ~ 21mp with a Cannon Macro EF 100mm 1:2.8 USM lens, set to autofocus. Lighting was provided with a Canon 580 EX II flash set to Manual 1:2 power. The flash unit was used off camera held oblique to the bite pattern. Camera settings were at the manual exposure of 1/200th @ f16-32, 100 I.S.O. with the white balance set on Flash. Large

JPEG format imaging process consisted of converting RAW images in Adobe Photoshop CS5 (cropped to 4x4 inches) and then calibrated to 1:1 at 300 ppi and saved in TIFF format. The calibration of the patterned injury proceeded by determining the total number of pixels within a known distance. The forensic photographer used the least distorted portion of the scale for the calibrations. A flat field lens was employed to help reduce optical distortion. At the lab, the images were calibrated to 1:1 and the analysis measurements were made using the technique previously reported for Tom's Toolbox©. Sorting and selection of the best image for each of the eight sites on the twenty-five pigs was accomplished. Since a scaled image of each dental arch was required to be analyzed separately by the semi-automated software, Tom's Toolbox©, a total of four hundred scaled digital images were calibrated at 300 dpi, duplicated and saved as working images in TIFF format. Those patterns which registered all six of the anterior teeth were considered complete, while those which registered only some of the anterior teeth were classified as partially usable. A third category, unusable, was assigned to those patterns which lacked sufficient detail. Duplicate working files were created for each of the investigators to independently measure the characteristics available. The duplicate working files were uploaded into the semi-automated computer application, Tom's Toolbox©, where they were measured by Investigators 1 and 2. The data was saved in an electronic data log.

Findings

The inter-observer agreement between Investigator 1 and Investigator 2 in the measurement of the 50 Coprwax™ exemplar patterns using SAS software was 0.984, showing an extremely high consistency when measuring widths of tooth patterns in an

American Dental Association (ADA) accepted dental bite registration material. Determination of the inter-observer agreement in measuring tooth widths of patterns registered in porcine skin was calculated with SAS software resulting in a correlation of 0.716.

Measuring the intersecting angles as a means of determining an additional dental characteristic has not previously been utilized in pattern research. The intersecting angles formed between incisor teeth identified as A and B, A and C, A and D, B and C, B and C and D were identified and compared to the corresponding angles from original data of the known population data set patterns. The correlations between bitemarks in porcine skin compared to the known measurements of the 469 dental models were ranked from 1 to 469. Each unknown model could only be ranked once as either 1 or some other number between 1 and 469. For Investigator 1, 84.6% of the measurement's showed that their true models were ranked in top 10%. For Investigator 2, 85% of the measurements showed that their true models were ranked in top 10%.

Pearson's correlation identified 2 and 5 ranking as number 1 by researcher 1 and 2 respectively when ranking from 1 to 469. In considering additional characteristics, correlations between a bite mark and its true dental model were highly ranked. For example, 10 out of the 143 (Investigator 1) and 13 out of the 156 (Investigator 2) were within in top 1%. Additional results can be interpreted similarly. All show a better performance than random with p-values < 0.0001. (Random in a statistical description indicates that selecting models until a match is made is not possible). Outliers were calculated using an N =469 to represent the population data. A calculated mean and

Edited 10/11/13

standard deviation was recorded as ± 2×SD. Width and angle calculations revealed more outliers than considering width alone or angles alone.

To verify the initial statistical model of analysis, a second statistical model using distance metric analysis was employed. The Distance Metric family of models computes a distance in an *n*-dimensional factor space from a Sample (unknown pig pattern) to each member of the known population data set of 469. The score for a particular member of the Distance Metric family of models is the percentage of the Population that is closer to the specific sample (pig pattern) than the correct matching Target member of the population data set from which the sample image was made. In three (3) (2.9 %) of the 102 Sample images scored, only 1% of the Population was closer to the Sample than the Target; 16 (15.7%) of the Samples found their Target within 5% of the Population; and 23 (22.5 %) of the Samples found their Target within 10% of the Population. For this data set, the Distance Metric Model performs a little better on the upper jaw Samples than on the lower jaw Samples, and there was no appreciable difference in performance using the Sample and Population measurements of each researcher. In summary, in more than 20% of the Samples in this study, the Distance Metric Model finds the Target within the closest 5% of the Population. In more than 6% of the Samples, it finds the Target within the closest 1% of the Population. This demonstrates that it is possible to determine scientifically that a given Sample must belong to a very small (e.g., 5% or even 1%) proportion of the Population.

Conclusions

The production of a legible pattern replicating the teeth in skin depends upon multiple factors in addition to the substrate and the mechanism. Firm substrates such as

Edited 10/11/13

cheese, soap, plastic and leather, to cite several media, register dimensions best. The mechanism of creating the bitemarks in skin can be divided into two categories; dynamic and static. Dynamic distortion occurs when there is movement by either or both victim and assailant. Static distortion is less common and in the opinion of the authors occurs more often in the pattern of the lower teeth because it is not fixed in position as is the maxilla. A variable even in a static bite is the degree of elasticity in the skin and the inability to capture the exact dimensions of the teeth. The evidentiary value of the injury pattern is related to the amount of distortion in the bite mark (injury pattern). However, even a distorted bite mark may still contain measureable characteristics that provide evidentiary value. When agreement exists in the analysis of a pattern between all examiners, there still is a need for a scientific basis and level of confidence for their opinion.

Prior to this report, to accomplish the frequency distribution of the dental characteristics, making an individual's dentition distinctive, a series of studies were instituted to establish a methodology for quantification dental characteristics in both two and three dimensions. This was initially utilized to build a data set of seven dental characteristics. Additional research confirmed the reliability of measurements, testing both intra-operator and inter-operator agreement in analysis. The initial quantification of width, damage, angles of rotation, missing teeth, diastema characteristics (spaces) and arch width were subsequently augmented by a study of the displacement of the anterior teeth, labially or lingually, from the individual's physiologic dental arch form. Later a three-dimensional study of the position of the incisal edge of the anterior teeth on the horizontal (Z) plane was conducted. This study adds a practical application to this data set. It incorporates a geometric approach to determining the angles of rotation of the four maxillary and mandibular incisors. This concept utilizes the measurement of the angels at the intersection of the extended incisal lines, projected through the mesial and distal markers of each of the incisors.   This method of measuring rotation of the intersecting angles of the incisal lines is beneficial for several reasons. It eliminates subjective establishment of an X (horizontal) axis. It is also more universal. One or more teeth may be missing or indistinct. If two or more anterior teeth can be identified (e.g. tooth 7 and 9), computation of the angle of the intersecting incisal lines can still be determined. This method of establishing tooth rotation also provides an expanded scope of search analysis, since it includes two additional characteristic items. In the earlier studies when an x axis could be established from the presence of posterior teeth, it was possible to determine four angles of rotation using a standardized and adjustable x/y axis template. With the alternate method of the intersecting angles formed by the incisal lines, it is possible to measure six angles of rotation.

Although the actual width of the pattern of the incisor in skin may be less than that of the known source, the angle of rotation remains a constant. Most significant in predicting probability of a correlation to a target in the population data set will be the presence of outlying angles of rotation. This procedure adds four additional characteristics to statistically calculate the probability of correlation between the unknown and a known source.

The interpretation of the combination of quantified dental characteristics making up the initial two-dimensional data set, also utilized the data obtained in the three-dimensional study, since the anterior teeth are not always all at the same level of eruption on the horizontal plane (Z plane). In knowing this, questions regarding whether certain teeth are present or missing in a patterned injury cited by past investigators could be addressed. This groundwork research is only the beginning. By establishing a scientific template continued research should continue to develop this relatively new scientific approach to pattern analysis.

Whether dental characteristics are reliably replicated in a bite mark in human skin is the current challenge. The scientific validation of the correlation of bite marks, or tooth patterns to their origin, in the opinion of the authors, predictably will be established by statistical probability. That is, how many outlying characteristics demonstrated in a pattern(s) would reliably predict the probability of another individual in the population having the same combination of dental characteristics? For those images of the bitemarks that include all six anterior teeth, or several teeth that enable the investigators to insert all ten, or at least some of the markers from Tom's Toolbox©, measurements of distances and angles could be determined, saved, calculated, stored in an internal data set ranked in percentiles. This application establishes outliers for those specific characteristics for a data set that includes males between the ages of 18 and 44 years in the State of Wisconsin. This is not to imply that only males bite. Women children, and animals also bite others and even inanimate objects. In the personal experience of the authors, perpetrators of human bites in violent crime are predominately males 18-44 years of age. This and limiting the number of samples required was the rationale for our original study to that group. The study is meant to augment the established guidelines of the American Board of Forensic Odontology. It should not be used in testimony or legal proceedings.

Introduction

The National Academy of Science (NAS) report *Strengthening Forensic Science in the United States: A Path Forward* (2009) challenged the forensic science community to develop comprehensive reforms in using scientific methodology, guidelines and standards for the analysis and reporting of an examiner's conclusions. [1] This research is the culmination of ten years of applied science, studying bite mark analysis. It demonstrates that human bite patterns can be replicated in porcine skin under some conditions. The study also illustrates that analysis and recovery of meaningful data in these patterns can be accomplished using a software application that recognizes the systematic placement of markers and calculates angles and distances (Biometrics). This pattern analysis software was developed by the investigative team in earlier research. This basic drag and drop marker program was developed as a tool for the forensic image specialists and forensic odontologists' use in the evaluation of patterned injuries. It also would initially assist crime laboratories and investigating agencies in determining whether there is the need for the expert services of a forensic odontologist to interpret the patterns.

Statement of Problem

The scientific basis for bite mark analysis has been questioned. The National Institute of Justice awarded a three-year research grant to determine whether the patterns of human teeth can be replicated in skin and correlated to the source with a degree of probability. Additionally a proposal was made to develop a template for forensic odontologists and forensic imaging specialist in ascertaining the forensic value of the pattern. This template is not rigid in the software and materials that future researcher use. It is only a general plan (template) for future researchers to follow to expand the testing of a scientific method in the replication and analysis of bite marks in human skin. Prior research provided the accuracy and validation of a software application (Tom's Toolbox©) which demonstrated it was reliable, repeatable and consistent with acceptable scientific methods. A blind study was designed and used to determine the statistical probability of a best fit. Two hundred patterned injuries were produced in porcine skin, documented by scaled digital images and analyzed. Two statistical models were used to establish the probability of a correlation of a replicated pattern with the known model in the population dataset. Confidence intervals and levels are reported. Factorial conclusions are presented based on the demographics of a male population between the ages of 18 and 44 years in the State of Wisconsin.

Literature Review

In prior research, the investigative team developed a means of measuring and quantifying seven specific characteristics of the human dentition. [2] This established a population dataset of 469 samples from males 18 – 44 years old that closely mirrors the distribution of the ethnic population in the State of Wisconsin. [3] The methodology employed was validated by testing repeatedly for reliability and accuracy. [4] Inter-operator and intra-operator agreement was studied and found to be extremely high. The result of repeated testing demonstrated that the methodology and protocol have a confidence level of 95% and a confidence interval of ±1.55.

The methods of bite mark analysis, used over time, have ranged from:

- Simple observation;
- The direct comparison of a known dental model to the injury pattern;
- Hand-traced outlines on clear acetate of a model of known dentition;
- Radiographs of Barium filled wax imprints of the known model as an overlay;
- Photographic transparent prints of images of the teeth utilized as an overlay;
- The use of optically scanned images of the dentition to produce overlays in Adobe Photoshop®
- Computer assisted analysis.

All of these techniques have their limitations, which include the viscoelasticity of skin, distortion from movement, photographic distortion and many other problems that are frequently cited and are well known to forensic examiners. Although these problems can occur, bite mark patterns may still provide details which have value. It is also important to point out, though most bite marks involve those observed in human skin; human tooth patterns have been recovered from inanimate objects and analyzed by the authors, e.g. kid gloves, automobile visors and steering wheels, a soft burrito, a bar soap, a wad of chewing gum and an apple.

An additional study of a seventh dental characteristic, quantifying the displacement of anterior teeth from the physical or native curve of each dental arch, was subsequently conducted and published. [5]

To establish the amount of displacement of the teeth, a baseline was necessary. Testing was conducted to determine whether an ellipse, a Bezier curve, or polynomial curve would provide the best fit. A third degree polynomial curve was determined to be the most appropriate. An algorithm was written for the ten markers to be placed in a 1:1 scaled image of the anterior teeth. The markers were placed at the center of the contra-lateral canine teeth to serve as the anchors and a marker was placed at the center point of each of the four incisors. This generated a third degree (best fit) polynomial curve. Based on this technique of establishing a baseline which follows the physiologic curve of the specific jaw and from which measurements could be made, the investigators were able to quantify displacement in labio-version or linguo-version, a seventh individual dental characteristic. It was also possible in this study to again establish inter-observer and intra-observer error rates. .

Adding to the data of the pattern reflecting width of the incisors which may not all be on the same horizontal (Z) plane, a three dimensional study was undertaken. Advances in Cone Beam Computer Technology (CBCT) have established that linear measurements in 3-D imaging programs are statistically no different than using a direct digital caliper measurement method considered by orthodontists to the most accurate for these measurements. [6] [7] [8] [9] This three-dimensional, expanded data set on the width of the eight incisors in 0.5 mm incremental “slices” on the Z plane has been reported and published. [10]. Three-dimensional, digital Imaging communication in Medicine (DICOM) images were obtained from the scanning the dental stone models, utilizing Cone Beam Computer technology. These DICOM format files were then converted to an STL format. The width of the incisors in the three-dimensional images of the dentitions were measured on the "z" plane using Materialise® MiniMagics© software. (Figure 1)

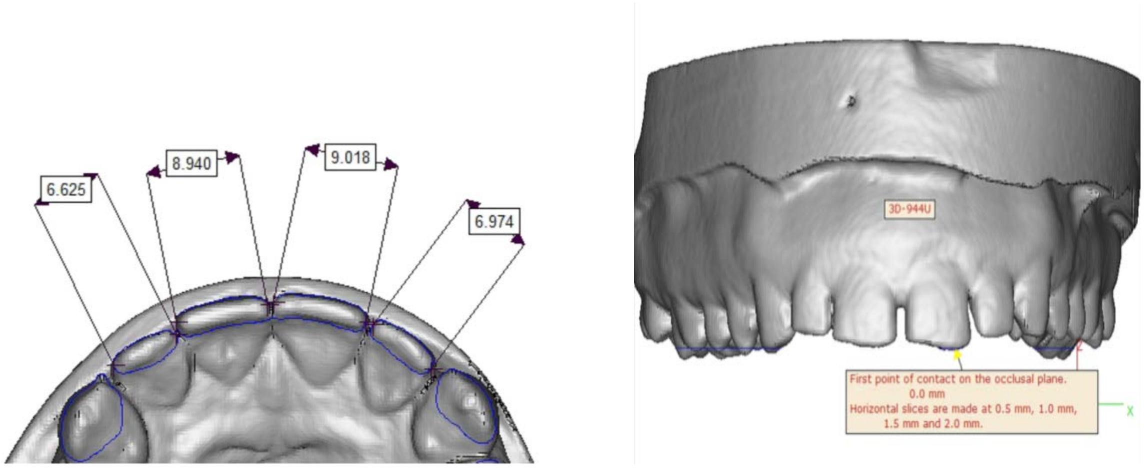

Figure 1. Illustrates the width of the maxillary incisor teeth measured at 1.0 mm above the first point of initial contact on the horizontal (Z) plane using the MiniMagics© software.

An additional paper providing data on the correlation of arch width with ethnicity was published.[3] McFarland, Rawson, Barsley and Bernitz have all contributed to the quantification of individual characteristics of the human dentition and identified problems that existed regarding a statistical evaluation of individuality. [11] [12]13] [14] None of these papers included a data set of significant statistical size, compared to that developed by the current research team, nor did they include the analysis in the third dimension on the (Z plane).

Statement of Null Hypothesis

It is not possible to replicate bite mark patterns in porcine skin, nor can these bite mark patterns be scientifically correlated to a known population data set with any degree of probability.

Methodology

To obtain pattern characteristic correlations using a two-dimensional comparison of the unknown injury patterns (bite marks) to the known population data set, this study proposes to:

- Demonstrate whether it is possible to replicate, in vivo, known dental pattern characteristics (bite marks) in porcine skin.
  - In a blind study, use 50 models randomly chosen from 500 previously measured Castone® models to be prototyped in a hard polymer by sintered stereolithography (SLS),
  - Document, analyze the patterns recorded and develop analytic models which could establish the statistical probability of a correlation of any of the pattern registrations in the pig skin (pattern replication), would have to the authors' population data set of known characteristics.
  - Determine the circumstances; area of the skin, the number of pounds force (lb^f) and duration of the applied force which produced identifiable and measureable patterns.
  - In the absence of the other landmarks to establish an X axis, develop modifications of Tom's Toolbox©, enabling the measurement of the angles of

rotation of individual incisor teeth using the intersection of an extended incisal line, based on Euclidean geometry. Determine the range of pounds force (lb^f) produced by males, age 18 – 44 when creating a bite mark.

- Based upon all of the preceding, establish a basic template and technology for the forensic imaging specialist and forensic odontologist to use in analyzing and evaluating patterned evidence.
- Provide a scientific template for future research with an enlarged population database and more sophisticated imaging software.

Establishing bite forces

Bite force measurements in the central incisor area were established using a mini load cell from Omega Engineering, Inc. (One Omega Drive, P.O. Box 4047, Stamford, Connecticut 06907-0047), serial no. 291633 and recorded using a precision Bridge Excitation voltage, V_B. = 5.000 VDC. Subjects were instructed to bite as hard as they could over a 10 second period. The initial output offset voltage, V_{OS}, mV and the resultant maximum load cell output reading Vout, were mV recorded. All output voltages were corrected by subtracting V_{OS} and subsequently converted to actual biting forces in pounds force (lb^f). These conversions were accomplished using manufacturer calibration data (5-Point NIST Traceable Calibration) that accompanied the load cell. The results were plotted graphically using lb^f for the y axis and individual results on the x axis. Those results that fell outside two standard deviations were discarded. The resulting N of 31 was totaled and the average recorded.

Edited 10/11/13

In replication of patterns utilizing the pounds force (lb^{f}) citied in the literature by Anusavice, the authors determined that the 20 to 30 lb^{f} cited in the text was insufficient to produce the degree of tissue injury commonly observed in bite marks. [15] In order to ascertain whether this observation was valid, an additional study was developed.

Caucasian male dental students who volunteered to participate were examined. The initial IRB protocol limited participation to 50 individuals. Nineteen individuals were dropped, making the final total thirty-one. Three were eliminated because they exceeded the 22 to 32 age range of dental student volunteers cited in the IRB protocol. Sixteen were excluded because the initial design of the load cell force transducer produced evidence of hysteresis or fade. A modification in the design of the bite force transducer included an intervening strip of stainless steel and a vinyl index to guide the lower incisor directly over the location of the load cell. The average bite force for males between the ages of 22 and 32 years with N=31 was 62.5 lb^{f} or 278.01N. This is significantly higher than the average bite force reported by Anusavice [15]. The actual minimal to maximum forces generated was 19.2 lb^{f} to 132.1 lb^{f} or 111.21 N to 587.61N**.**

The force was calculated using an Omega™ model LCKD-100 load cell force transducer sandwiched between two parallel wooden tongue depressors with a metal plate directly over the sensor to avoid compression [Figure 2], that could result in hysteresis in evaluating applied force. Sample results are shown in [Table 1] which indicated an average of 62.5 pounds force, with a maximum of 132.1 pounds force and a minimum of 19.2 pounds force for a group of volunteers on a given recording date.

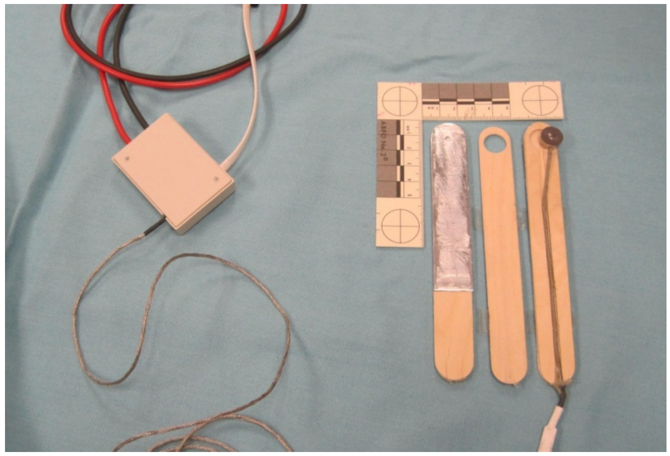

Figure 2. An exploded view of the prototype bite force transducer using the Omega™ model LCKD-100 mini load cell, to determine the range of pounds force (lb^f) generated by twenty males ages 22 to 32. The insertion of a sheet of stainless steel controlled hysteresis.

Edited 10/11/13

Bite Measurements

Dates 14 December 20 2012,4 Jan 2013,11 Jan 2013

Load cell Serial No.-291633

By: D Jeutter and T. Radmer

Bridge Excitation V= 5.000

SoD Room 106D

Note: Stainless steel inner layer and incisal alignment guide added to transducer

Subject Code Number	Subject age	Initial offset V_{out} mV	Load cell V_{out} mV	Actual Bite Force #F	Notes
617	29	0.146	9.475	132.1	
34	26	0.142	2.76	37.1	
519	26	0.142	1.78	23.2	
409	24	0.137	3.57	48.6	
225	26	0.154	5.76	79.4	
599	27	0.137	3.47	47.2	
41	25	0.137	3.7	50.5	one incisal restoration
218	26	0.134	5.66	78.2	
415	24	0.134	3.98	54.5	
259	27	0.141	3.164	42.8	
398	24	0.138	4.378	60	
945	39	0.142	1.863		dropped
797	25	0.147	5.46	75.2	
322	34	0.144	3.66		dropped
380	25	0.146	1.5	19.2	
540	31	0.134	5.66	78.2	
67	25	0.136	4.1	56.1	
199	25	0.117	8.097	112.7	
52	23	0.028	6.355	89.6	
376	26	0.032	6.849	96.5	
326	25	0.059	3.78	52.7	
35	27	0.046	6.13	86.2	
496	23	0.047	6.399	89.9	
662	27	0.04	3.95	55.4	
591	25	0.045	3.78	52.9	
749	25	0.039	2.146	29.8	
804	25	0.057	2.56	35.4	
303	26	0.048	4.96	69.6	
576	25	0.62	1.826	25	
530	33	0.45	5.08		dropped
51	27	0.044	5.721	80.4	
643	22	0.067	4.84	67.6	
850	22	0.064	3.769	52.5	
568	26	0.09	3.98	55.1	
88	24	0.042	3.96	55.5	
318	26	0.036	5.22	73.4	
			Sum	2062.5	
			average 31 subjects	62.5	

Table 1. Illustrates the range of bite force (lb[f]) that can be generated by thirty-one males age 22–32 in the region of the maxillary incisors. The average (mean) was 62.5 lbs/Force.

Procedure for measuring bite mark patterns.

Using in-vivo porcine skin to research patterned injuries in human skin has had widespread acceptance in the medical and dental literature.

A literature review of the use of a porcine model in bite mark research and analysis provides only two examples when using the terms bite mark and porcine skin as search criteria [16], [17]. Past and current literature compares the porcine skin model closely with human skin [18].

In previous studies, a template for the measurement of individual characteristics of the human dentition in two-dimensions was established by the authors [4]. This included the development of an original software application, copyrighted as Tom's Toolbox©. [Figure 3] This software is a semi-automated software application using a palette of ten markers which when inserted by the analyst in a scaled digital image, calculates distances and angles based upon the Pythagorean Theorem. It is licensed to governmental and non-profit organizations by Marquette University The markers are inserted in specific locations on a scaled digital image of the bite mark at the starting and ending point of the areas to be measured. The software recognizes the location of each of the markers by column and row. It first performs a quality control procedure to assure that all of the markers have been inserted and are in the correct order. It then calculates distances and angles of rotation.

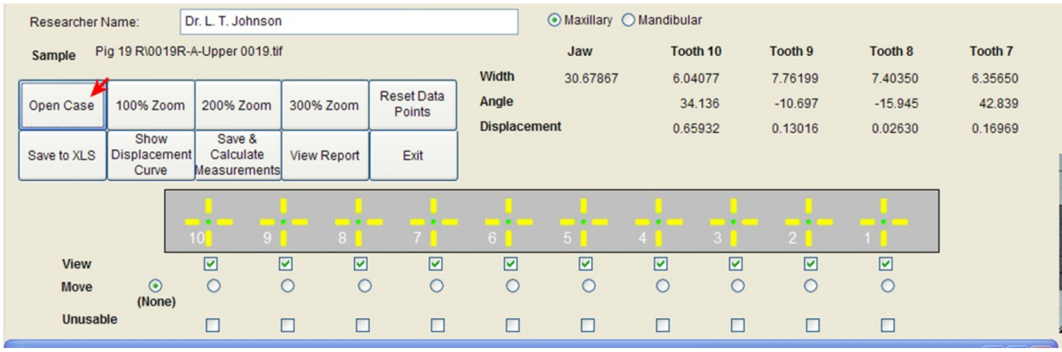

Figure 3. The tools panel used in pattern analysis. The arrow indicates the tool used to open a case for analysis in Tom's Toolbox©i

Calibration of the FlexiForce® Sensors

A method of providing standardized forces, duplicating the human bite forces was addressed using FlexiForce®, sensors (0-100 lbs.), mounted in a custom designed recording pattern replication device. The FlexiForce® sensor is a versatile, durable piezo-resistive, force sensor that can be constructed in a variety of shapes and sizes. The device senses resistance inversely proportional to an applied force. It has a patented ultra-thin (0.008 inches) flexible printed circuit that senses contact force. It acts as a force sensing resistor in an electrical circuit. When the sensor is not loaded, resistance is very high and when the force is applied the resistance decreases proportionately. The FlexiForce® sensors were coupled with an application that measures force-to-voltage in a circuit. [Figures 4, 5, 6 and 7].

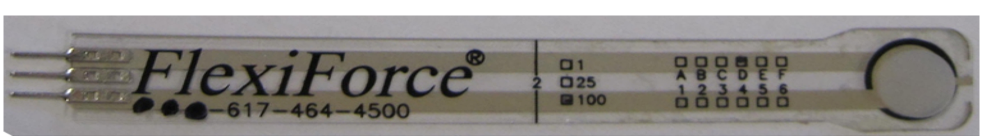

Figure 4. Illustrates a 0-100 lb. FlexiForce® sensor with the supplied silastic pressure button, which resulted in fade, (hysteresis) when recording applied force.

Edited 10/11/13

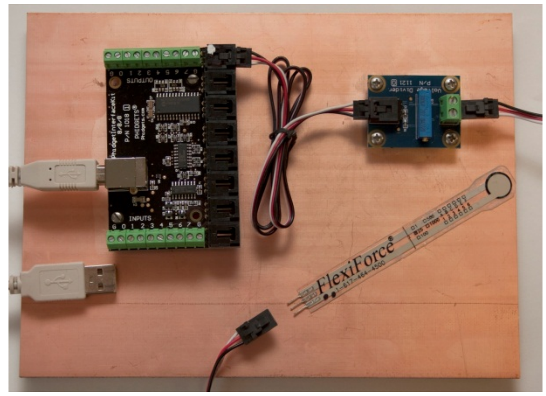

Figure 5. Omega LCKD 100 mini load cell. **Figure 6.** The Phidgets data system

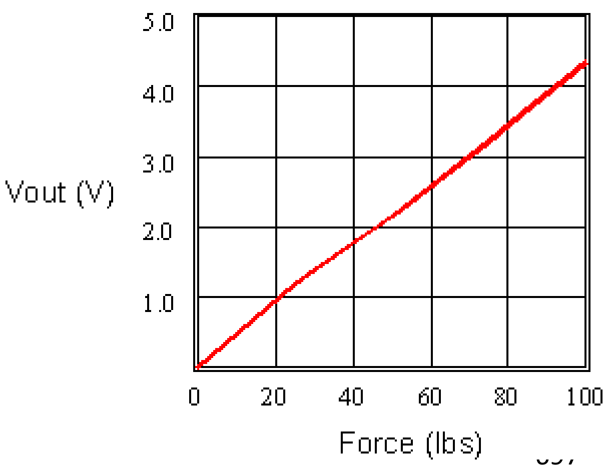

Figure 7. Illustrates the FlexiForce® Sensor response graph www.trossenrobotic.com [20]

FlexiForce® Transducers (FFT) [20] were incorporated into the apparatus to measure the applied force, as described elsewhere.[21] These thin transducers are in the Force Sensing Resistor (FSR) family that changes resistance from open circuit at 0 lb^f, applied forces to a resistance that progressively decreases as additional force is applied. The resistance output is linear (±3%) with applied input force. The FFTs were calibrated *in situ* after mounting in the bite replication model. Calibration of each FFT in the pattern replication device was accomplished by inserting a commercial subminiature industrial compression Omega load cell model LCKD-100 with a capacity of 0 to 444.82 N (Omega Engineering Inc., Stamford, Connecticut, U.S.A., 06907-0047) in series with the

Edited 10/11/13

FFT while forces were applied. This is the same Omega load cell which was used directly in the tongue depressor bite force transducer, measuring the dental students' bite force. Each bite replication model's calibrations data was recorded in spreadsheets.

The FFT selected for bite force measurement, (0-100 lb. FlexiForce® resistive sensor) is manufactured by Tekscan, Inc. (model A201 E) 134 Tekscan Inc. 307 West First Street, South Boston, Ma., U.S.A. 02127-1309). It is basically a flexible plastic film printed circuit approximately 0.22mm thick by 102mm. long by 14 mm. wide. The sensitive force registration area is 0.375 inch (9.53mm) diameter.

The FFT was incorporated into a voltage divider circuit to obtain a voltage change that is proportional to the change in applied force. This voltage divider is part of a commercial data acquisition system, a 1120 FlexiForce Adaptor that was purchased from Phidgets, Inc. (Phidgets® Inc. Unit 1, 6115- 4th Street S.E., Calgary, Alberta, Canada T2H 2H9) leading into a Phidgets Interface Kit 8/8/8 P/N 1018. [figuren8]

The complete Phidgets data acquisition system consisted of a voltage divider, a precision voltage reference source, an Analog to Digital Converter board (ADC), USB interface and a laptop computer [figure 9]

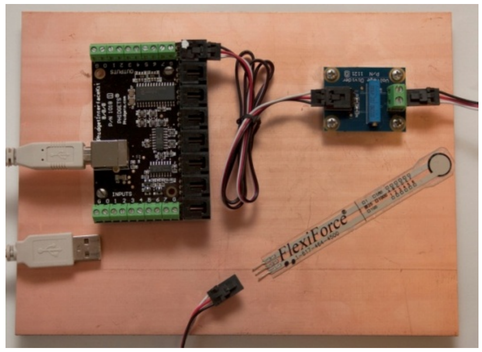

Figure 8. The Phidgets / FlexiForce® transducer (FFT) system block bridged to a display and storage application custom designed for the PC laptop by the team's IT manager.

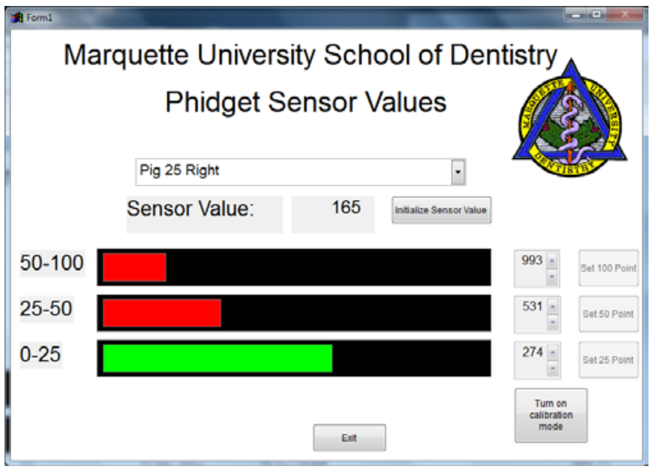

Figure 9. A screen capture of the computer display of the application which provides a visual and an audible indication of the applied $lb^{f\ force}$ and the duration it was applied. The application also creates a complete log of the session.

Model duplication and mounting

The dental stone models proved to be brittle and porous and were unsuitable for this study. They would not withstand the forces applied [figure 10].

Edited 10/11/13

Fig. 10. Illustrates one of the original dental stone models used to create the population data set in prior research.

Fifty sets of upper and lower dental stone models were randomly selected from the population data set which was established and reported in previous studies. [2][3][5][10] The statisticians for the project created a blind list of models for the investigators numbering the fifty pairs of models in random order, using the identifier of Pig 1R and Pig 1 L to identify the first two sets of models that were selected from the data set of N= 469. Subsequent models were similarly identified in alpha numeric fashion by pig numbers 1-25. The fifty hard polymer models were produced by stereolithography, using a 3M™ ESPE Lava COS scanner and Lava Software 3.0. (3M ESPE Divisions, 3M Center, St. Paul, MN 55144-1000, U.S.A.).

The method determined to be the most expeditious for the duplication of the models was to prototype them in a durable resin capable of withstanding the forces to be applied. The dental stone models were scanned in STL format files utilizing the 3M™ Lava COS® scanner, a chair-side optical scanner originally designed to capture a three-dimensional image and directly generate a prototype model of the dentist's prepared tooth for laboratory procedures. It replaced the necessity for an indirect dental impression. (3M™Corporation, St. Paul, MN). (Figure 11A and 11B)

3M™ESPE Lava COS® scanner [11A]   Screen capture of a scanned model [11B]

Figure 11 A and Figure 11 B. Illustrates the 3M™ ESPE COS chair side optical scanner and a screen capture of a three-dimensional image of the dental stone models in STL format.

After the models were prototyped by the 3M™ Corporation using sintered stereolithography (SLS) the prototyped models were returned in a hard 3M™ proprietary polymer with sheer strengths equal to or exceeding bite forces of the natural dentition of 20-25 pounds force. [15] (Figure 12)

Figure 12. Illustrates the 50 blind prototyped models returned by the 3M™ Corporation.

Edited 10/11/13

A protocol standardizing the replication of dental characteristics in porcine skin was developed using a modification of an apparatus reported in an earlier study. [19][21] The models were mounted on a modified Irwin™ welder vise grip, using dental laboratory acrylic. (Figure 13) (Figure 14) A means of recording the applied pounds force (lb$^{f)}$ and the duration of the applied force in a log was developed. By incorporating a force sensor, (FlexiForce® 100 lb. sensor), a Phidgets device to bridge the sensor to a notebook computer running Lab View software, an auto-recording, pattern replication device was designed. The models were articulated utilizing a custom jig to standardize the mounting of the models on the 50replication devices which were required.

The models were mounted, using a custom mounting jig developed to align the dental models in a normal occlusal relationship.

Figure 13. Illustrates the mounting jig on the left. The upper mounting base in the center showin the dowels permitting the vertical travel, yet maintaining the inter-arch relationship of the models. On the right, a FlexiForce® sensor is shown inserted directly over the anterior teeth.

Edited 10/11/13

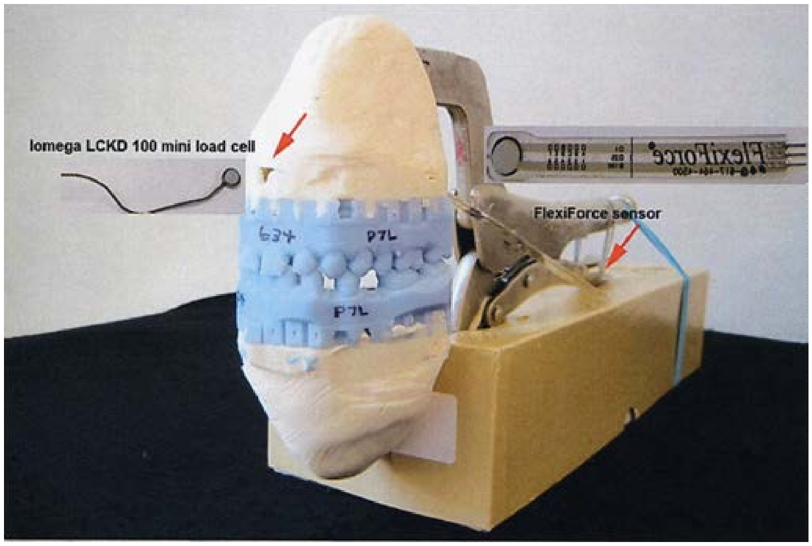

Figure 14. Illustrate a completely assembled pattern replication device with a channel above the maxillary incisors for the introduction of the Omega load cell for the calibration of the FlexiForce sensors in each of the 50 pattern replication devices.

The mounting was designed so the upper dental model does not adhere to the upper acrylic base. Its position is maintained, but allowed to travel vertically, using ten parallel brass dowels, keyed to the upper model's anatomic relation to the lower model. The dowels were placed in the maxillary molar, premolar and canine locations before the upper model is mounted to the C-clamp with the laboratory acrylic. Tin foil substitute was used to permit the model to be separated later for the insertion of the omega load cell for calibration of a FlexiForce® pressure sensor. This step was necessary to prepare the replication apparatus for the calibration of each FlexiForce® sensor.

Biomedical Engineering Laboratory Procedures

Once dismounted from the C-clamp device, a flat bottomed, one half inch recess was created in the base of the maxillary model with a Forstner 1/2 " drill bit to accept a

Edited 10/11/13

mini load cell used to calibrate the FlexiForce© sensor in each of the 50 pattern replication devices. (Figure 15)

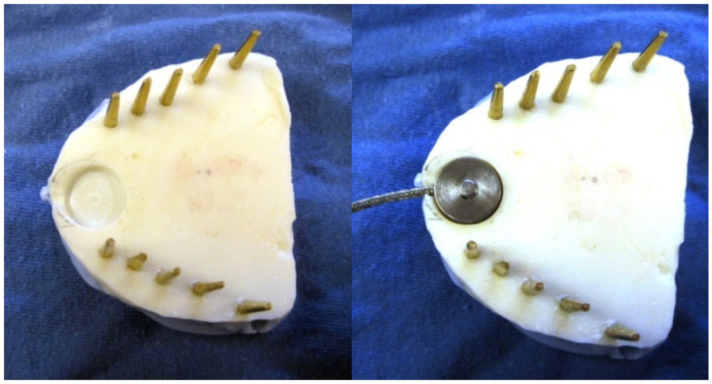

Figure 15. Illustrates the recess created for insertion of the Omega model LCKD-100 mini load cell.

To mate the Omega mini load cell and the pressure sensing area of the FlexiForce© sensor and minimize hysteresis, a button was machined from a 3/8th aluminum rod, the exact diameter of the pressure sensing area of the 8 inch FlexiForce® 0-100 lbs. resistive force sensor (Trossen Robotics, 2749 Curtiss Street, Downers Grove, IL 60515). This ensured that the force transmitted through the incisal edges of the maxillary incisors were compressing the entire area of the force sensor and that the force was directed perpendicular to this contact point. (Figure 16)

The calibration procedure was carried out by connecting the installed FlexiForce® Transducer (FFT) to the Phidgets data acquisition system and verifying its operation on the connected laptop computer, running the software application. (Lab View). Next, the load cell was placed in the replication apparatus, arranged mechanically in series with the embedded FFT sensor so that both transducers experienced the same biting force. Force was applied at 0, 25, 50 and 100 pounds-force increments then removed at 50, 25 and 0 pounds force increments. Corresponding data from the FFT and the load cell were taken at each force increment and stored in a time and date stamped computer file for each of the 50 models and 50 corresponding pig locations.

Initial experience with the calibration of the FFT revealed that a means of applying force explicitly to its 0.375 inch diameter force sensing area with an uncompressible interface is essential. The rigidity of the button material and its diameter are critical to avoid fade or hysteresis in the recording of sustained forces. The solid aluminum discs, machined from aluminum rod, provided the least fade in the pressure force measurements when the anterior dentition was loaded for 15 seconds and provided the desired FFT adaptation to the pattern replication device. The button thickness was selected to properly couple the force generated by the anterior teeth sensing area on the FFT to the button sensor of the mini load cell. The resultant remaining hysteresis in our measurements was that contributed by the FFT at <4.5% of full scale.

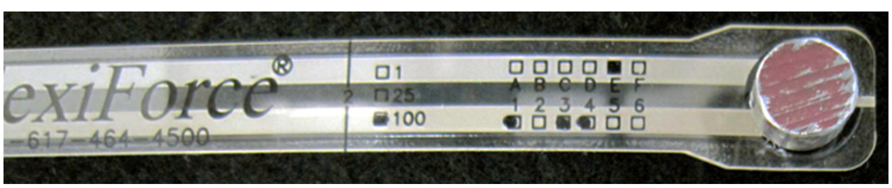

Figure 16. Illustrates the 0-100 lb. FlexiForce® sensor with the custom machined aluminum pressure button.

Procedures were developed early on to enable initial testing, evaluation and calibration of the FlexiForce® sensors. This allowed for an informed design of the interface buttons, the signal conditioning circuits for the load cell and the Phidgets system for FFT data acquisition. Bench testing was done by placing the load cell

Edited 10/11/13

mechanically in series with the FFT in a small hobby vise with careful alignment of the FFT, button and load cell. (Figure 17)

Bench testing was done by placing the load cell mechanically in series with the FFT in a small hobby vise with careful alignment of the FFT, button and load cell. (Figure 17)

Figure 17. FFT transducer calibration was accomplished in series with the Omega load cell in a small bench vise.

This simple means of applying a variable force to the FFT and the load cell allowed for an informed incorporation of the FFT sensors into the bite models as well as for system development.

The Omega model LCKD-100 load cell force transducer was specifically selected for this force measurement and calibration efforts because of its small size. The 0.5 inch diameter by 0.25 inch thick load cell came with a five point NIST documented calibration with a ±0.25% accuracy, sensitivity of 2mV/V (i.e.: ratio metric), full scale output of 100 pounds-force (444.82 N), linearity of ±0.25% of full scale output, ±0.25% hysteresis with respect to full scale output, and a repeatability of ±0.10% repeatability with respect to the 100 pound-force scale capability. The transducer is temperature compensated. This precision load cell provides a force proportional voltage output signal to a custom designed amplifier signal conditioner. These specifications ensured that the load cell could be used as a precision calibration reference for the FFT sensors.

The load cell's internal strain gauge sensors are connected in a full 350 Ohm bridge. The bridge was excited with a stable, precision 5 VDC and the differential bridge output signal was connected to the input of a custom designed signal conditioner. The signal conditioner was configured with two stages of gain, regulated power supply voltage and a novel automatic zero calibration. The two operational amplifier (OP AMP) gain stages provided a total gain of A_v =200V/V. The two gain stages included an instrumentation Amplifier (IA) cascade with a non-inverting gain amplifier for signal conditioning. The IA has a voltage gain of A_v =100. A negative feedback circuit (A to D and D to A converters) was added to the circuit to automatically cancel input offset voltage from the load cell bridge prior to recording data.

The output from the load cell conditioning circuit is given by:

- V_{out}=Load cell sensitivity[mV/pound –force] x signal conditioner voltage gain [V/V]
- The load cell sensitivity is provided by the manufacturer: e.g. S = 7.1 mV at 100 pounds-force (or 71µV per pound-force).
- For example, it the applied force is 50 pounds-force, the load cell output is 3.55 mV. So the system output is: V_{out}= 3.55mV x 200 V/V= 710mV.

Calibration was performed on each instrumented bite model prior to its

Edited 10/11/13

use. (Figure 18A, 18B)

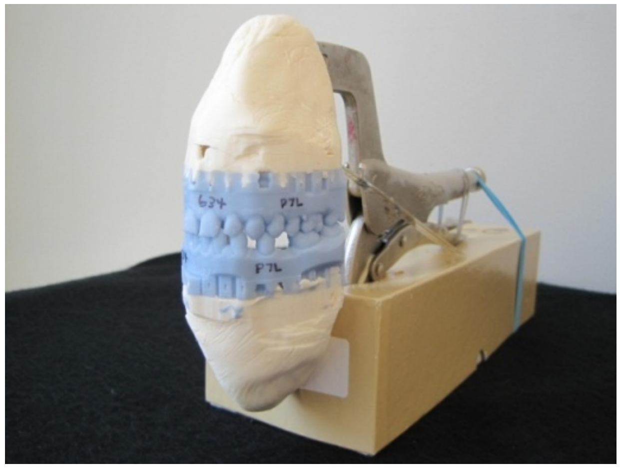

Figure18A. Depicts an articulated replication device.

Figure 18B. Upper model travels vertically on ten brass dowels.

Animal Laboratory Procedures

Animal research sessions were conducted in accordance with the standards of the *Guide for the Care and Use of Laboratory Animals* (8th edition, National Academies of

Sciences, 2011) and approved by the Medical College of Wisconsin, Institutional Animal Care and Use Committee (IACUC). (Figure 19)

Figure 19. Illustrates the Biomedical Resource Center's large operating suite at the Medical College of Wisconsin where the animal research was conducted.

Mixed-breed young pigs, weighing 30-40 kg were obtained from a commercial breeder and acclimated in the large animal laboratory research facility for a period of at least 2 days before the laboratory procedures were performed. Anesthesia was induced with a combination of tiletamine/zolazapam (Telezol®, 4.4 mg/kg) and xylazine (2.2 mg. /kg) administered intramuscularly. Following induction, an endotracheal tube was placed and hair from the anatomical sites of interest was removed using a commercial hair clipper, razor, and/or depilatory cream. To conserve body temperature, animals were placed on heated pads on the surgical tables and covered with towels and a PolarSheild® Emergency Survival blanket (RothCo 3015 Veterans Memorial Highway, Ronkonkoma, and New York 11779-0512). The pigs' body temperatures were maintained between 36.2 and 39.3 degrees C. Using a rectal thermometer, two veterinary technicians monitored the pigs' body temperature and respiration.

The mean procedural temperature was 38.1C (36.2C – 39.3C). The mean low 36.2C (33.9C – 37.0C) and the mean loss was 1.8C (0.2C – 4.3C).Following animal preparation, a surgical plane of anesthesia was maintained using isoflurane administered through the endotracheal tube using a precision vaporizer and compressed oxygen. Basal anesthesia was augmented as needed in some animals with pentobarbital administered intravenously.

The four designated sites to receive the patterned injury were the lateral aspects of the upper hind limb/thigh, abdomen/flank, thorax, and shoulder/upper forelimb of the animals. (Figure 20)

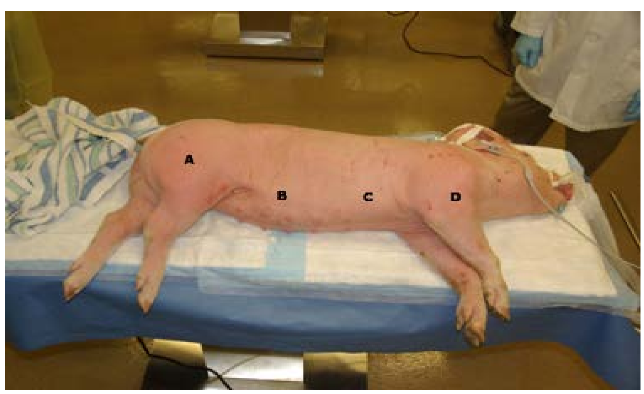

Figure 20. Depicts the four standard sites selected on each side of the animal for the replication of bite marks (patterned injuries).

Because the surface and sub-surface features of porcine skin, *Sus scrofa*, vary with the anatomic location, much the way they do in human skin, multiple sites were chosen to receive the replicated bite. In their confocal laser scanning microscopy of porcine skin in wound healing, Vardaxis et al, have demonstrated that the success of such studies is dependent on control and standardization of the injury infliction protocol. [22] The size of the pigs used (20-40 kg) and the skin structure made the production of patterns possible at similar anatomical locations bilaterally, with observations and photography made 15 minutes post-infliction to introduce as little variation between areas on the same animal. There were a total of eight (8) replicated bites on each animal. The pounds force (lb^{f}) necessary to produce the patterns were standardized from 50 to 99 lbs. and were continuously monitored using the described FlexiForce® sensor connected to a force-to-voltage circuit and data acquisition system.

Each application was held for a minimum of 5 seconds to a maximum of 15 seconds, or the estimated time that a human with normal musculature and tempro-mandibular joint function can maintain a sustained force without muscle fatigue. [23] [24]

Forensic Digital Photography

The patterned injuries were created with the custom designed, semi-automated, recording pattern replication apparatus. The injuries were digitally photographed at 1:1 scale (life size) by a highly experienced forensic photographer, beginning 15 minutes after their creation, using a Canon™ EOS 5d Mark II, ~ 21mp with a Canon Macro EF 100mm 1:2.8 USM lens, set to autofocus. Lighting was provided with a Canon 580 EX II flash set to Manual 1:2 power. The flash unit was used off camera held oblique to the bite pattern. Camera settings were at the manual exposure of 1/200th @ f16-32, 100 I.S.O. with the white balance set on Flash. Large JPEG format imaging process consisted of converting RAW images in Adobe Photoshop CS5 (cropped to 4x4 inches) and then calibrated to 1:1 at 300 ppi and saved in TIFF format. Calibration and correcting for perspective distortion can be two different issues. Even though they are related, they are separate entities. An orthogonal object may not be 1:1 (or calibrated).

The calibration of the patterned injury proceeded by determining the total number of pixels within a known distance. Once determined, that known pixel count can be provided into the image size box with the known distance set and the calibrated resolution, for that distance, will be revealed. That resolution is used to determine the exact size of the image by placing it into the image size box with all three known (length, width and resolution) "locked". When perspective distortion is introduced (and most all systems/lenses have some - optical and linear) the calibration may (most will dependent upon amount) become skewed. The forensic photographer used the least distorted portion of the scale for our calibrations. As an alternative, there is a correction for this distortion in Photoshop (especially if it is slight). The other option was to be certain that our scale is perfectly flat upon the pig and the camera plane is parallel and perpendicular. The forensic photographer employed a flat field lens to help reduce optical distortion. At the laboratory, the images were then calibrated to 1:1 and the analysis measurements made using the technique previously reported for Tom's Toolbox©. [28]

Image Selection

A total of 800 digital images were exposed, four for each of the 200 sites, exposing digital images from all four compass points following the guidelines of the Scientific

Edited 10/11/13

Working Group on Imaging Technology (SWGIT) [25] and the guidelines for bite mark evidence of the American Board of Forensic Odontology (ABFO) [26].

Sorting and selection of the best quality image for each of the eight sites on the twenty-five pigs was accomplished. Since in Tom's Toolbox© a scaled image of each dental arch must analyzed separately by the semi-automated software, a total of four hundred scaled digital images were calibrated at 300 dpi, duplicated and saved as working images in TIFF format. Those patterns which registered all six of the anterior teeth were considered complete, while those which registered only some of the anterior teeth were classified as partially usable. A third category, unusable, was assigned to those patterns which lacked sufficient detail.

Image analysis and measurement

Duplicate working files of the 200 images were created for each of the investigators to independently measure the characteristics available. The duplicate working files were uploaded into the semi-automated computer application, Tom's Toolbox©, where they were independently measured and the data saved in an internal log.

The semi-automated software application, Tom's Toolbox©, utilizes ten markers which are inserted in a specific order into the image at the starting and ending points of the pattern to be measured. The application recognizes the location of each marker by column and row, to calculate distances and angles of rotation.

The usable and partially usable images were measured for arch widths, tooth widths, angles of rotation, and spacing. The application provides the operator a check box option for indicating whether any or all of the markers for measuring dental characteristics cannot be placed. (Figure 21) Tom's Toolbox© saves the measurements in a data set in an internal log. From the data saved in the internal log a software application can then generate a report on the frequency distribution of the pattern in the population dataset.

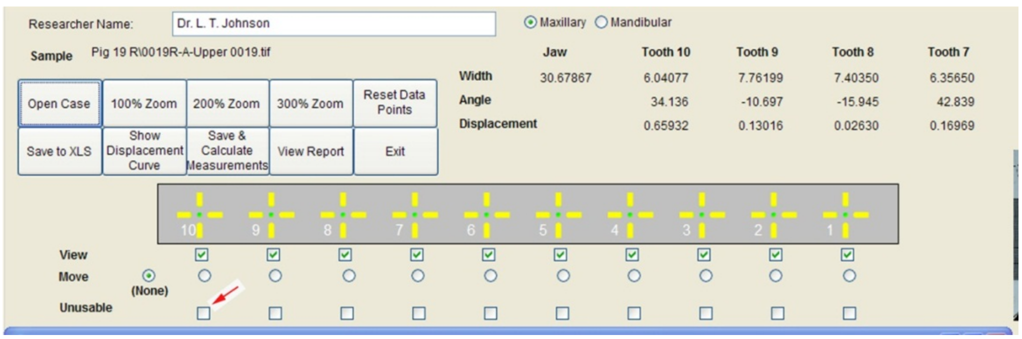

Figure 21. The arrow indicates the location of the control button used to indicate that a specific site in the bite mark pattern image where a Toolbox marker could not be inserted at that site.

The measurements from each examiner's image files were saved in a log within Tom's Toolbox© and then transferred to an Excel spreadsheet for statistical analysis. The spreadsheet is programmed to check for data entry errors.

Quality control was accomplished by identifying and correcting any errors or omissions in measurement or missing image files and a revised spreadsheet was created.

Once the investigators were satisfied that all of the data in the spreadsheet was correct, it was transmitted to the collaborating statisticians for statistical analysis. Statistical programs were created by the consulting statisticians from the Medical

Edited 10/11/13

College of Wisconsin and Marquette's University's College of Engineering, Department of Electrical and Computer Science. These resources were utilized to develop models enabling the determination of the probability that measurements of the individual characteristics in the injury patterns could be correlated with a degree of probability to the known model in our population data set, testing the stated hypothesis of pattern replication.

Image selection

In the process of evaluating and sorting the suitability of the best 200 image, the inter-observer agreement on suitability was highest for those considered to be complete (these images exhibited recognizable sites for the insertion of all ten of the markers in Tom's Toolbox©). Both examiners agreed there were 87 of the 200 upper arch patterns determined to be complete. Agreement differed somewhat in that examiner 1 determined 116 lower arch patterns were considered complete, while examiner 2 determined 110 were complete. (Table 2)

	Investigator 1 Lower	Investigator 2 Lower	Investigator 1 Upper	Investigator 2 Upper
Number of Images Considered Partially usable	17 (8.5%)	39 (19.5%)	17 (8.5%)	34 (17%)
Number of Images Considered Completely Unusable	67 (33.5%)	51 (25.5%)	96 (48%)	79 (39.5%)
Number of Images Considered Complete	116 (58%)	110 (55%)	87 (43.5%)	87 (43.5%)
Total	200	200	200	200

Table 2. Illustrates the extent of the intra-observer agreement in the selection of images for analysis.

An observation related to the finding of image patterns that was considered completely unusable, is whether the production of the pattern was static or dynamic. There is little or no movement in a static bite and consequently there is a more distinct pattern registered.

Determination of Angles of Rotation

In the earlier studies of complete patterns of the entire dental arch, angles of rotation were computed for each of the four anterior incisors. Computation was based on an x-axis established by the principal investigator. To establish an x-axis, an adjustable template consisting of both an X and a Y member was developed, which would superimpose a reference line (x axis) between the distal most points of the contra-lateral first molar teeth. The automatically adjusted Y axis bisects the X axis and establishes the midline of the arch. Adjustment to the specific landmarks on the image was accomplished in Adobe Photoshop, using the Edit > Transform > Scale, or >Rotate. (Figure 22A and Figure 22B)

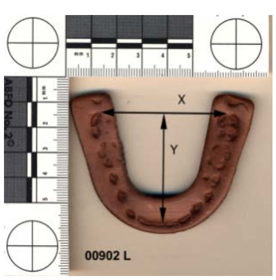

Figure 22A. The X Y axis inserted in a scaled image for measurement.

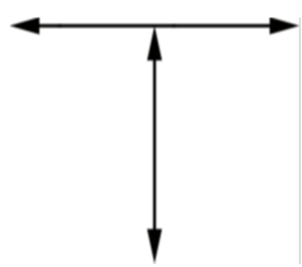

Figure 22B. The adjustable X Y template used to establish the X axis.

In the current pattern replication research project, only the registrations of the six maxillary and mandibular anterior teeth were imprinted. It then became necessary to

Edited 10/11/13

establish an alternate method of determining angles of tooth rotation, independent of the posterior dentition. This approach measured tooth rotation in relation to the intersecting angles of an extended line projected on the incisal edge of each of the four incisors. This was accomplished through a modification of the use Tom's Toolbox© and the absence of X and Y coordinates for the pixel marker placed for each tooth. The incisal line is defined as a straight line along the incisal edge of the incisor teeth, connecting the directly opposite mesial point to the distal most point on the tooth's incisal edge. The extension of this line intersects with an adjacent incisal line of the other teeth forming a measurable intersecting angle**.** The computed angle of intersecting lines based on all combinations of the four anterior teeth was recorded. Assuming the four anterior teeth are A, B, C, and D, the computed angles of intersection would be: AB, AC, AD, BC, BD, and CD.

Recording force and duration

Using the SAS System and incorporating the Means Procedure, the electronic Phidgets logbook for the bite pattern replication study recorded 4684 points of data during the 25 sessions.

The mean recording for all points in which pressure was applied was 545.6, with a standard deviation of 278.7 within the range of pressures recorded for each event between 0 and 997.0 on the FlexiForce™ sensing device. Each of the FlexiForce™ sensors were bench calibrated for pounds force (lb^f) with an Omega™ model LCKD-100 mini load cell. Force versus Time was plotted for each pig location. As an example, Pig25_L_A (left side, pig 25, position A) is represented in figure23 and the resultant bite pattern can be seen in figure 24. Each of the 200 patterns was similarly correlated to the maximum force of the device over a period of 15 seconds.

start_side_site=Pig_25_L_A

Analysis Variable : value				
N	**Mean**	**Std Dev**	**Minimum**	**Maximum**
47	665.5531915	168.9966309	152.0000000	817.0000000

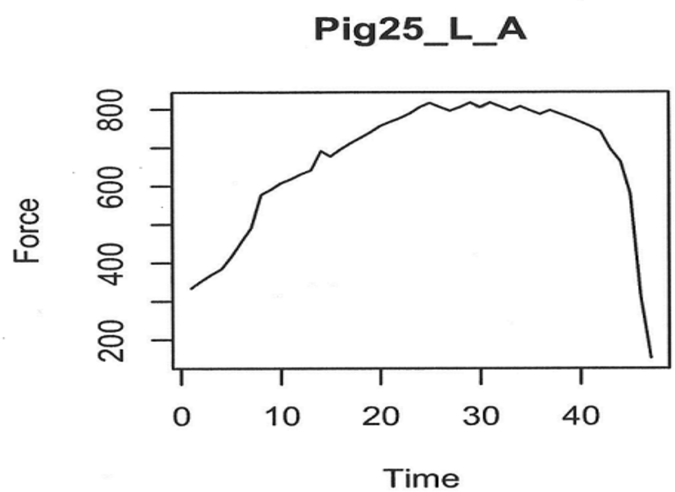

Figure 23. Analysis variable for pig number 25 left side, site A (hind limb) representing the mean force of 665.553191 Phidgets sensor reading with minimum and maximum loads over 15 seconds of maximum load force.

Figure 24. bite mark replication pattern for pig number 25L A (left side, position A) representing the mean force of 665.553191 Phidgets sensor reading with minimum and maximum loads over 15 seconds maximum load force.

Image analysis

Analysis using Tom's Toolbox© began once the images had been reviewed and selected. Of particular importance were the images and resultant forces producing them that led to a high level of inter- observer agreement. For example the patterns on Pig 19R appeared highly consistent with model 945, when a transparent overlay comparison was conducted. (Figure 25)

Edited 10/11/13

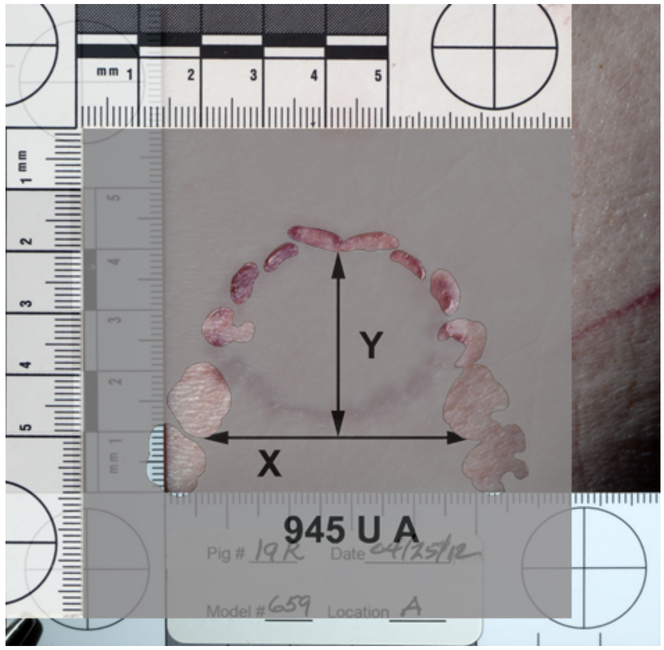

Figure 25. Illustrates the consistency of the pattern in dental characteristics in bite pattern 19R A and the population Target member 945 U A, using a computer generated semi-transparent overlay.

Consistency in all characteristics does not quantify the frequency with which the pattern occurs in the population. The strength of the correlation of model number 945 with pattern 19R, site A, required constructing statistical models. The resultant pixel placement and forces used to create the bite mark are illustrated in Figure 26A, 26B and 26C.

Figure 26A. Illustrates the placement of the measurement markers in Tom's Toolbox© for the maxillary incisors in the replicated bite mark for pig 19R, site A.

Edited 10/11/13

Analysis Variable : value				
N	Mean	Std Dev	Minimum	Maximum
58	784.7586207	101.9286490	551.0000000	997.0000000

Figure 26B. Depicts the force applied to produce the replicated pattern of the bite mark on Pig 19 R, site A

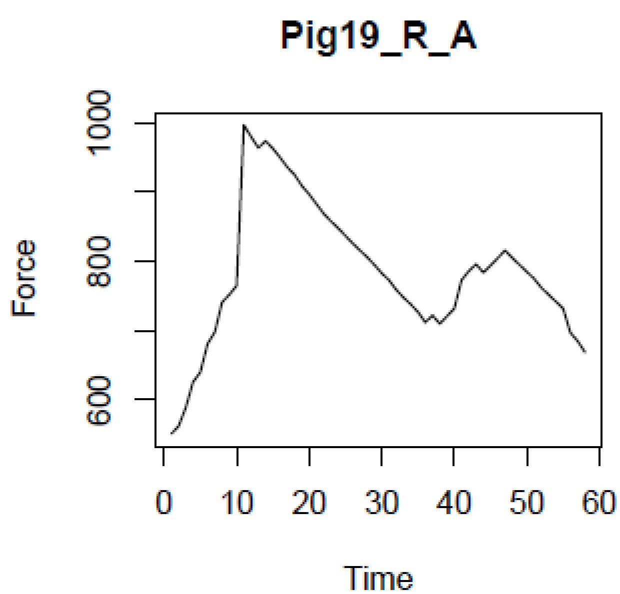

Figure 26C. Illustrates the FlexiForce scale recording of the force at 10 seconds to 25 seconds over the 60 second duration of the contact with porcine skin, Pig 19R, site A.

Edited 10/11/13

Results

Statement of Results Using Pearson Correlations

Statisticians evaluated width measurements for outliers utilizing two different analytic models. The results are found in table 3 for widths for standard deviation, median, minimum, and maximum width measurements in porcine skin for each tooth in each jaw.

	Mean ± StDev	Median	Minimum	Maximum
Upper				
Tooth 7	5.07 ± 1.05	5.15	2.12	7.88
Tooth 8	6.47 ± 1.16	6.66	2.29	8.39
Tooth 9	6.50 ± 1.18	6.70	2.86	8.87
Tooth 10	4.83 ± 1.07	5.00	1.22	7.80
Lower				
Tooth 23	4.97 ± 0.76	4.98	2.01	6.99
Tooth 24	4.74 ± 0.74	4.81	1.86	6.80
Tooth 25	4.64 ± 0.81	4.68	1.53	6.58
Tooth 26	4.91 ± 0.69	4.94	2.92	7.30

Table 3. The measured widths for each tooth in porcine skin expressed in millimeters

These widths were compared to the known widths established by the two investigators using Coprwax™ exemplars, a standard dental material for bite registration. An illustration of the results when searching for outliers in individual tooth widths is found in Table 4.

	Investigator 1	Investigator 2
Width and angle	23.42%	26.83%
Width	35.3%	50.1%
Angle	15.33%	10.21%

Table 4. The percentage of outliers in tooth widths plus angles, widths and angles only by investigators 1 and 2.

The viscoelasticity of the skin and the rebound that occurs restricted meaningful comparison when width was considered as a single characteristic. Analysis found that there were many bite mark patterns in porcine skin which exhibited several outlying measurements for each tooth**.**

The inter-observer agreement using SAS software between Investigator 1 and Investigator 2 in the measurement of the 50 CoprWax™ dental patterns was 0.984, showing an extremely high consistency when measuring widths of tooth patterns in CoprWax™, an American Dental Association (ADA) accepted bite registration material. Determination of the inter-observer agreement in measuring tooth widths of patterns registered in porcine skin was calculated with SAS software resulting in a correlation of 0.716.

Measuring the intersecting angles as a means of determining an additional dental characteristic has not previously been utilized in pattern research. The intersecting angles between teeth identified A and B, A and C, A and D, B and C, B and D and C and D were identified and compared to the corresponding angles recorded in the dataset. (Figure 27) The correlations between bitemarks in porcine skin compared to the known measurements of the 469 dental models were ranked from 1 to 469. For Investigator 1, 84.6% of the measurements showed that their true models were ranked in top 10%. For Investigator 2, 85% of the measurements showed that their true models were ranked in top 10%.

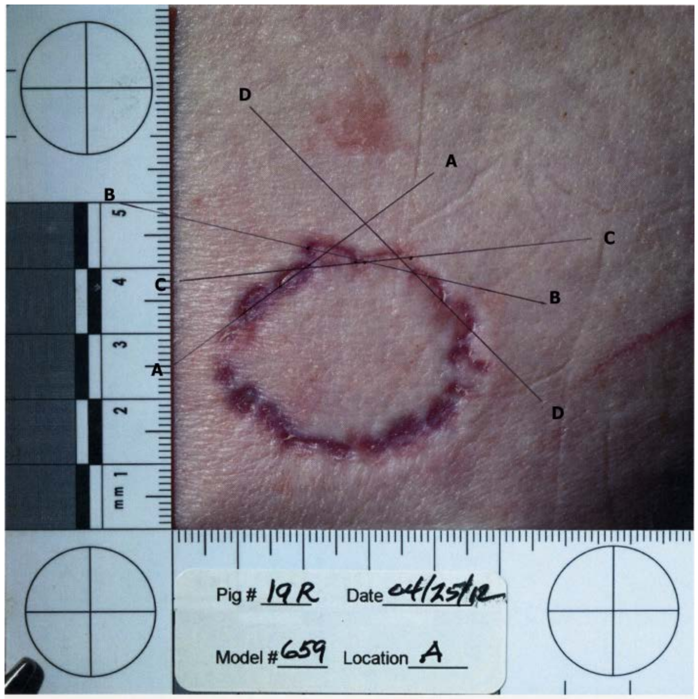

Figure 27. Illustrates the intersection of the extended incisal lines used to calculate the angle of rotation of the incisors. Outliers in these angles are used to quantify their occurrence in the sample population.

Based on the angle correlation, the list can be further narrowed for a comparison of porcine skin patterns and the set of models used to create true model candidates that had a confidence interval of 0.984.

The Pearson correlation was used to select a dental model based on the bite mark patterns. Two hundred bite marks were examined against 469 dental models. For each bite mark, 469 correlations with the dental models were calculated. Then, the 469 correlations were ranked from 1 to 469. The dental model having rank #1 correlation was the predicted model. Table 5 illustrates the results based on the all measurements, i.e., the width and the angles. 143 (Investigator 1) and 156 (Investigator 2) bite marks out of the 200 had at least one non-missing data entry. The data of the remaining 57 (Investigator 1) and 44 (Investigator 2) bite marks were completely missing (i.e., non-measurable). As can be seen in Table 5, five (5) out of the one hundred forty-three (143) (Investigator 1) and two (2) out of the one hundred fifty-six (156) (Investigator 2) selected correct dental models from the population data set. The models ranked number one in the data set were from separate members of the population. The P-values of less than 0.05 shows that this selection is better than random. For example, identifying 2 correct models out of the 156 (Investigator's Rank #1) shows a better performance than selecting a correct model completely at random (p-value = 0.0431), and 5 correct models out of the 143 case (p-value < 0.0001). Although correlation identified only 5 and 2 correct models, respectively, a lot of the correlations between a bite mark and its true dental model were still highly ranked. For example, 10 out of the 143 for Investigator 1 and 13 out of the 156 for Investigator 2 were within in top 1%. The rest of the results can be interpreted similarly. They all show a better performance than random (p-values < 0.0001).

	Investigator 1		Investigator 2	
	Proportion	P-value	Proportion	P-value
Rank #1	5/143	< 0.0001	2/156	0.0431
Top 1%	10/143	< 0.0001	13/156	< 0.0001
Top 5%	34/143	< 0.0001	36/156	< 0.0001
Top 10%	59/143	< 0.0001	54/156	< 0.0001
Top 20%	78/143	< 0.0001	76/156	< 0.0001
Top 30%	93/143	< 0.0001	105/156	< 0.0001

Table 5. The results of an analysis based on the measurement of both width and angles.

Table 6 shows the results based on width measurements only. 141 (Investigator 1) and 153 (Investigator 2) bite marks out of the 200 had at least one non-missing data entry. The data of the remaining 59 (Investigator 1) and 47 (Investigator 2) bite marks were completely missing. The correlations from Investigator 2 identified 3 correct models out of the 153, which is better than random (p-value = 0.0043). The correlations from Investigator 1 did not identify any correct models. Although Investigator 1 measurements did not show better performance than random selection, investigator 2's measurements showed a better performance than random (all p-values are less than 0.05).

Edited 10/11/13

	Investigator 1		Investigator 2	
	Proportion	P-value	Proportion	P-value
Rank #1	0/141	1	3/153	0.0043
Top 1%	0/141	0.4106	8/153	0.0002
Top 5%	7/141	1	15/153	0.0136
Top 10%	14/141	1	26/153	0.0067
Top 20%	32/141	0.4014	45/153	0.0060
Top 30%	41/141	0.8546	64/153	0.0019

Table 6. This table illustrates the investigators' difficulty in measuring incisor width only. This is due to the viscoelasticity of the skin, resulting in inaccurate measurements in distance.

Table 7 shows the results based on angular measurements only. 136 (Investigator 1) and 131 (Investigator 2) bite marks out of the 200 had at least one non-missing data entry. The data of the remaining 64 (Investigator 1) and 69 (Investigator 2) bite marks was not useable. . The correlations from Investigator 1 identified 3 correct models out of the 136, which is better than random (p-value = 0.0031). Although the correlations from Investigator 2 did not identify any correct models, some correlations between width measurements of a bite mark and its true dental model's width was still ranked high, which is better than random (p-value < 0.0001 for top 5% to top 30%).

Edited 10/11/13

	Investigator 1		Investigator 2	
	Proportion	P-value	Proportion	P-value
Rank #1	3/136	0.0031	0/131	1
Top 1%	10/136	< 0.0001	10/131	< 0.0001
Top 5%	30/136	< 0.0001	32/131	< 0.0001
Top 10%	46/136	< 0.0001	43/131	< 0.0001
Top 20%	75/136	< 0.0001	67/131	< 0.0001
Top 30%	87/136	< 0.0001	85/131	< 0.0001

Table 7. Illustrates the Investigators accuracy and consistency in an analysis based on angular measurements only.

Outliers were calculated using an N =469 to represent the population dataset. For each column (for example, the width of Tooth 24 or the angle of AB for upper tooth), a calculated mean and standard deviation was recorded as ± 2×SD.

Since the location of the observations is unknown, an iterative algorithm was used to find the best dental model to match the bite marks. To do this, all possible combinations between observations and dental models were examined. The best matched bite mark and dental model was determined by choosing the dental model and teeth marks that produced the minimum sum of absolute values of the differences between observations and measurements of the dental models. For example, when there were four observations of widths, a comparison was made using these four observed widths and all possible four measurements from all known dental models. Starting with the first tooth of each model, the absolute difference of teeth marks and models was compared.

This was then repeated around the entirety of the model until every combination of matching had been compared. The corresponding, dental model was chosen by producing the absolute minimum difference between observations and measurements from the dental models. For analysis, the outcome was whether the chosen dental model was correct, which created binary outcomes. Finally, generalized estimating equations (GEE) were employed to perform multivariate analysis of the predictability of the model selection.

In addition to the above multivariate analysis, further investigation of outliers such as missing teeth and significantly large/small measurements remain to be calculated beyond the scope of this investigation. In cases where there were outliers in observations, only dental models which had outliers were considered in order to perform the multivariate analysis as mentioned above.

Statement of Results Using a Distance Metric Model

A second scientific model was also selected to compare the population to the unknown injury patterns based on distance metric analysis. The Distance Metric Model addresses the question; W hat proportion of the population (CoprWax® exemplars) is similar to a specific sample image of an injury pattern on one of the pigs? The Distance Metric family of models computes a distance in an *n*-dimensional factor space from a sample (pig injury image) to each member of the population (CoprWax® images). The score for a particular member of the Distance Metric family of models is the percentage of the population that is closer to the specific sample, than the correct matching target member of the population from which the sample image was made as suggested by Figure 28.

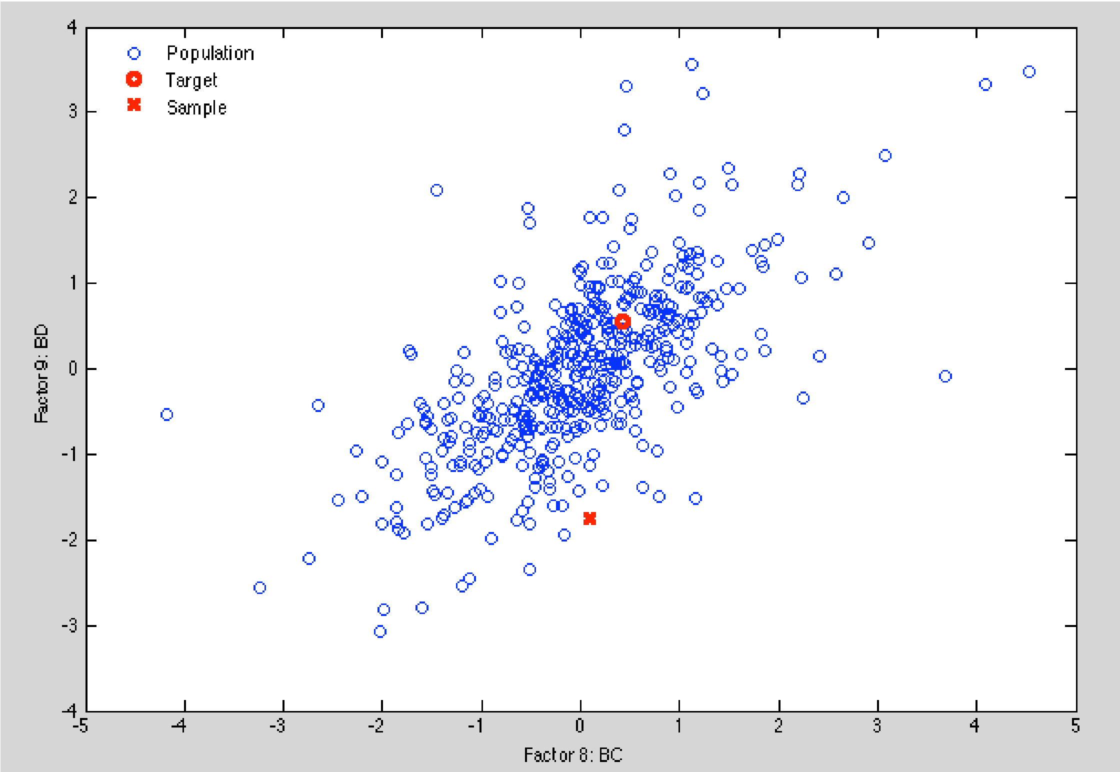

Figure 28. A visualization of the Distance in factor space from the Sample to the matching Target of the Population.

In Figure 28, "**X**" denotes a Sample image, and the heavy "**O**" denotes the matching target member of the population, represented in two of the angle measurement factors for upper jaw measurements by Investigator 1. In this view, it appears that most of the populati theon is closer to the sample than the target member of the population, but less than 5% of the population is closer to the sample than the target.

Edited 10/11/13

For analysis, data from 469 pairs of lower and upper jaws was provided and scored by two researchers independently. The factors scored were:

- Lower jaw: Tooth 23 width, Tooth 24 width, Tooth 25 width, Tooth 26 width, and angles AB, AC, AD, BC, BD, and CD.

- Upper jaw: Tooth 10 width, Tooth 9 width, Tooth 8 width, Tooth 7 width, and angles AB, AC, AD, BC, BD, and CD.

The lower jaw images had 7 missing teeth noted by the two independent researchers. The upper jaw images had 9 - 11 missing teeth. So that distances could be computed using multiple factors, each width and angle measurement was replaced by its corresponding z-score by subtracting factor means and dividing by factor standard deviations, ignoring missing teeth, and considering scores from each researcher separately

For analysis, 50 members of the population were selected as blind samples. Four separate simulated bite marks were made from each sample, giving 400 images each from lower and upper jaws. The two investigators independently scored the same 10 factors for each of the 400 images. Some of the population selected for the samples had missing teeth, but of the 800 teeth measured from each jaw by each researcher, between 276 and 420 (investigator 1 and investigator 2) missing teeth could not be distinguished in the images with sufficient clarity to assign factor measurements. Not all impressions were clear enough for analysis.

So that distances could be computed using multiple factors, each factor was normalized by subtracting population factor means and dividing by population factor standard deviations, considering scores from each researcher separately.

Before applying the Distance Metric Model, the data was visualized by looking at histograms for each factor (e.g., Figure 29), Normal Probability Plots (e.g., Figure 30), and scatter diagrams of each pair of factors (e.g., Figure 31). Figures 31, 32, and 33 show the plots for the upper jaw measurements from researcher 1; corresponding plots for lower jaws and for researcher 2 are very similar.

Edited 10/11/13

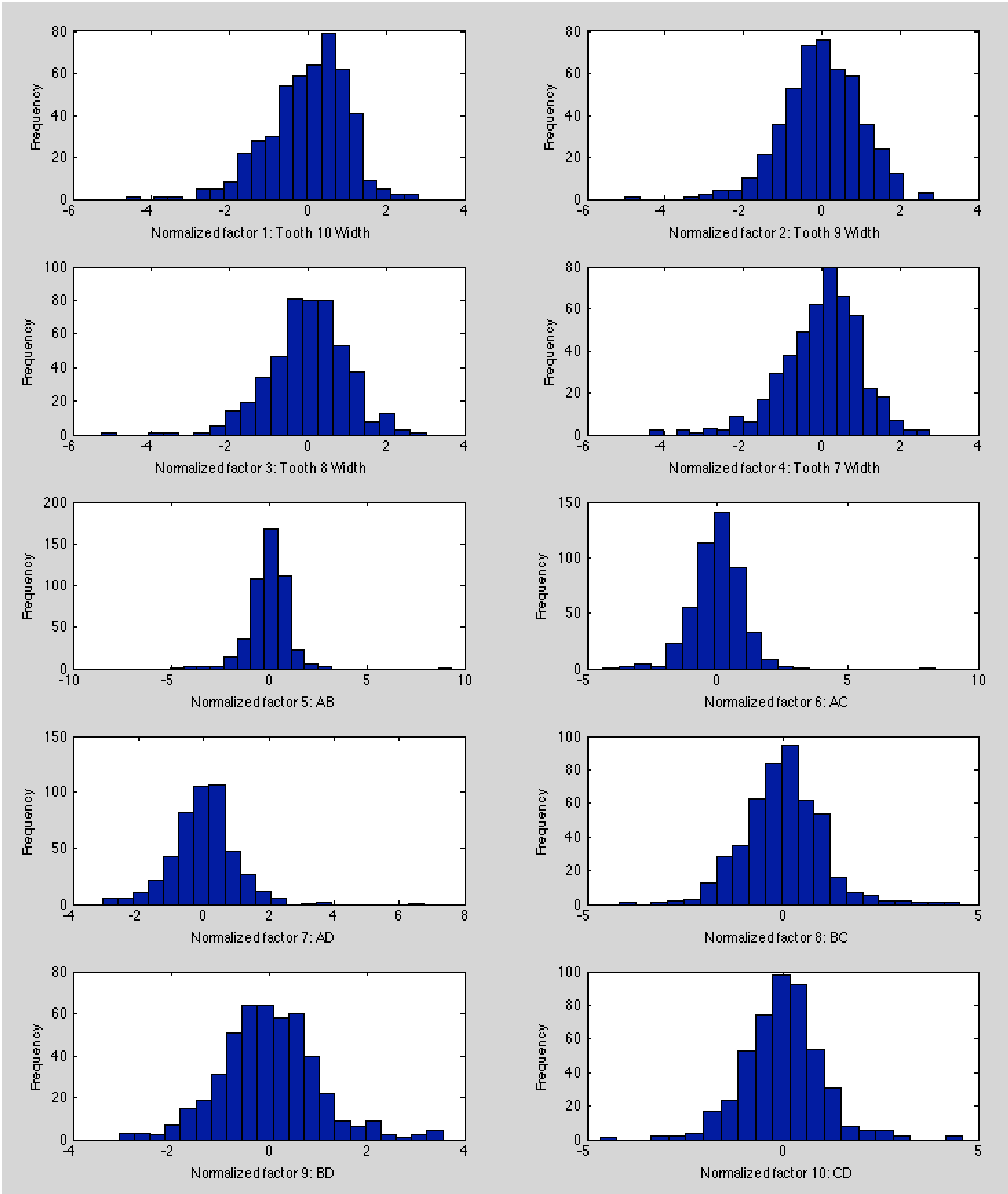

Figure 29. Histograms of ten normalized factors from upper jaw measurements by researcher 1. Distributions appear roughly bell shaped, but there are outliers.

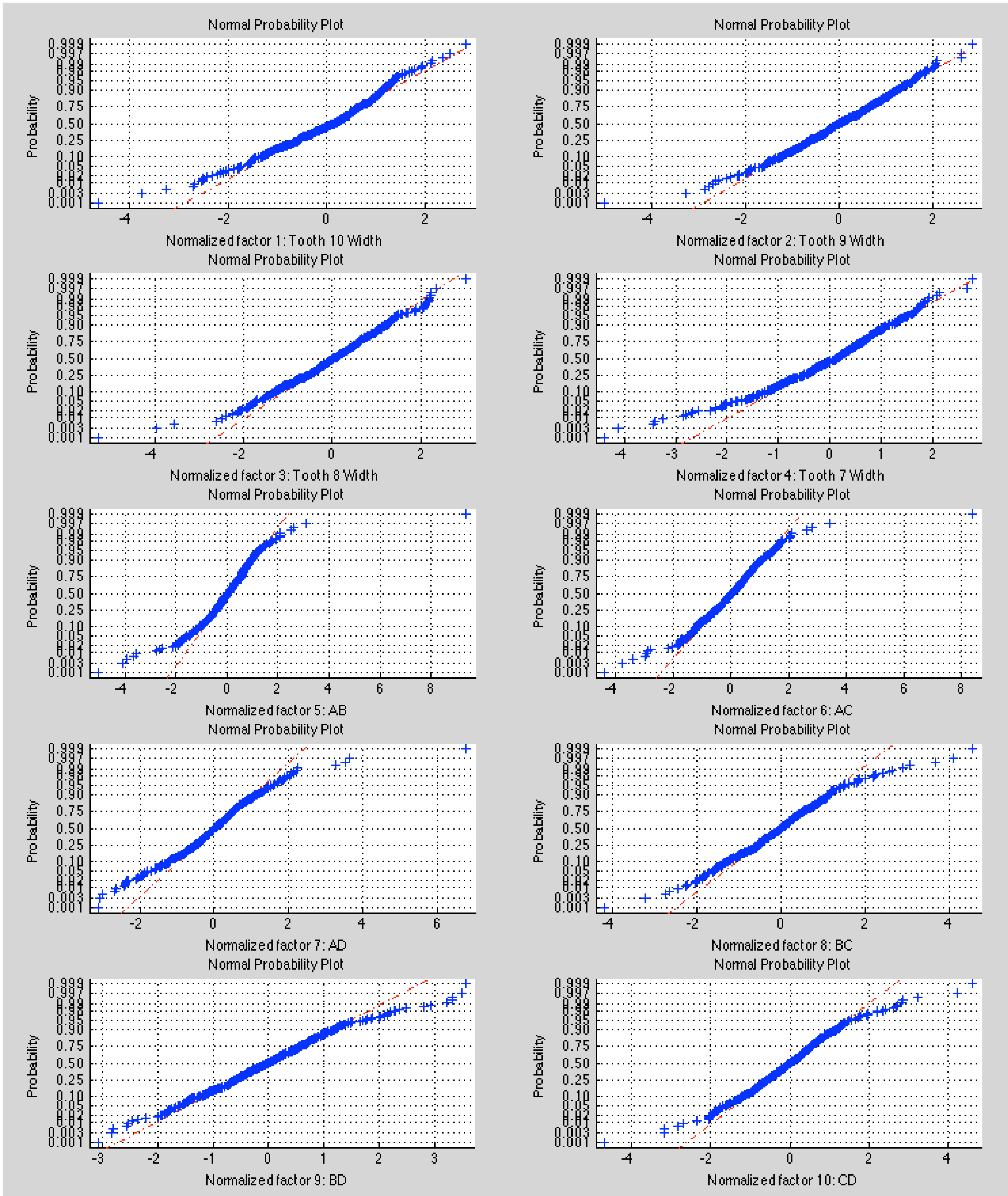

Figure 30. Normal Probability Plots of ten normalized factors from upper jaw measurements by researcher 1. If the observed distribution is normal, it follows the dashed red diagonal lines. Distributions of these factors tend to have thick tails, and some are skewed.

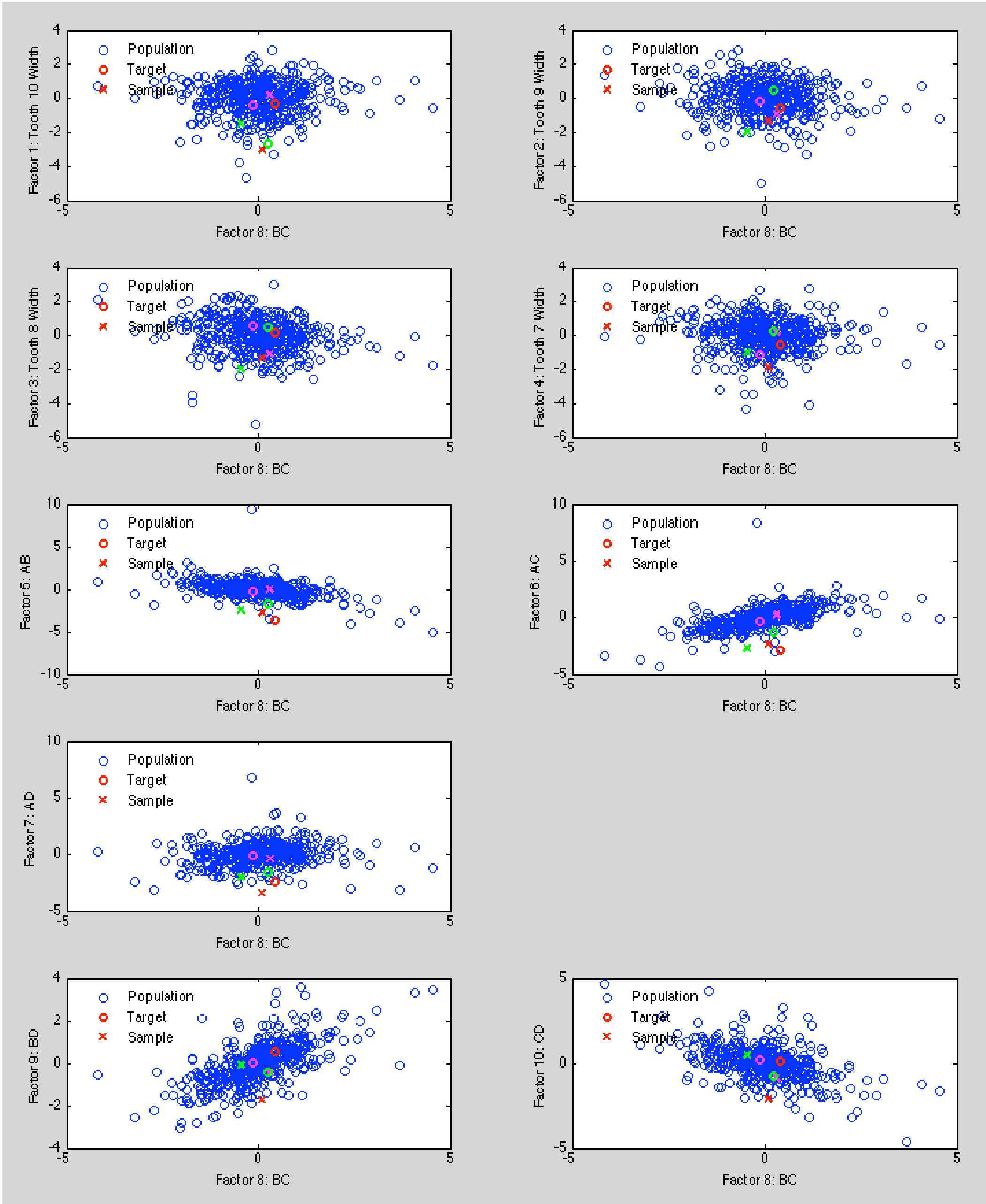

Figure 31. Scatter diagrams – Other factors vs. factor 8 (angle BC) for Population. Colored "**X**" are three Samples, with corresponding Target members of the Population marked "**O**"

For each Sample, the Distance Metric Model computes the distance (in *n*-dimensional z-score-normalized factor space) to each member of the population and then sorts the results in order of increasing distance. For each sample, the number of population members that lie closer to the sample than its corresponding target member of the population (the dental model that was used to create the sample image) was counted.

Figures 32 and 33 help visualize how the Distance Metric Model computes the distance between Samples and members of the Population. Figures 30 and 31 are enlargements of subfigures from Figure 29, showing scatter diagrams of factors 7 (angle AD) and 9 (angle BD), respectively, vs. factor 8 (angle BC). There are several outlier measurements, which provide good characterizations, but the choice was to focus here on more difficult Samples, marked with red, magenta, and green “X” (Samples) and “O” (Targets). The Distance Metric Model counts the number of Population members (blue “O”) that are closer to the Sample (“X”) than its corresponding Target (“O”). For these three pairs, the percentages are 4.8 %, 1.7 %, and 23% for red, green, and magenta pairs, respectively.

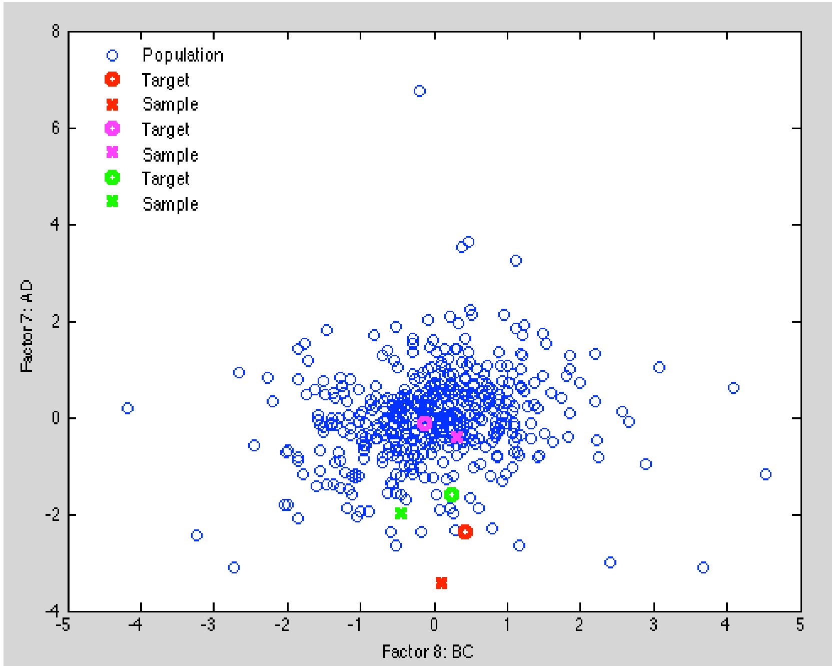

Figure 32. Factor 7 (angle AD) vs. factor 8 (angle BC) showing three Sample – Target pairs.

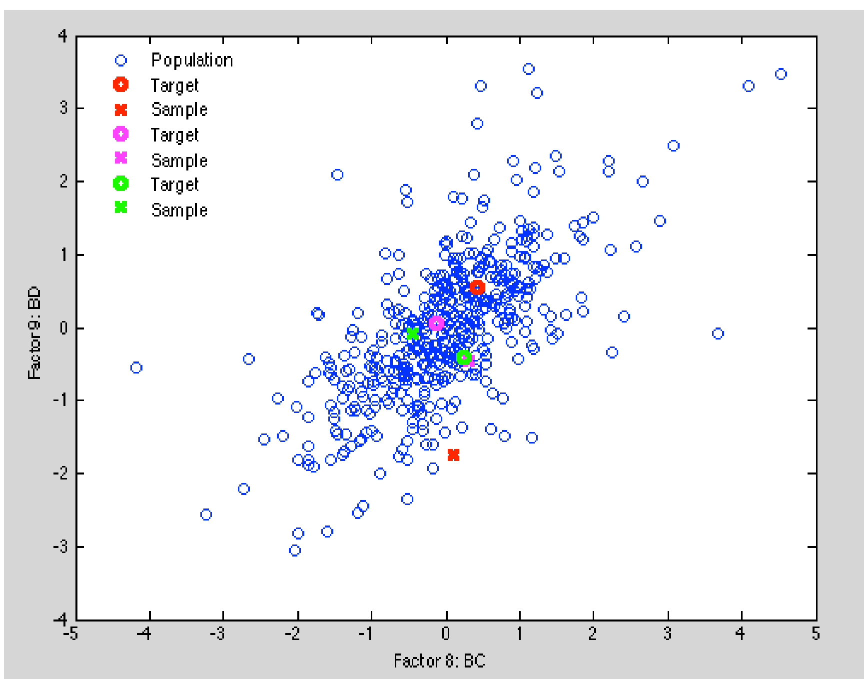

Figure 33. Factor 9 (angle BD) vs. factor 8 (angle BC) showing three Sample – Target pairs.

Edited 10/11/13

These figures illustrate the effect of measuring the distance in a high-dimensional factor space, rather than in the two-dimensional spaces. One pair of dimensions alone is insufficient, but by considering all factors, one may resolve pairs that appear widely separated in a single feature pair.

By having the 10 factors provided in the data set for the upper jaw Samples measured by researcher 1, we get the results shown in Table 8. Results for lower jaws and for measurements by researcher 2 are similar.

Average target percent: 39.1

Sample count: 102

Within 1% of population: 3, 2.9 % of samples

Within 5% of population: 16, 15.7 % of samples

Within 10% of population: 23, 22.5 % of samples

Table 8. The Percent of the Population closer to selected Sample than the corresponding Target for the upper jaw. Samples were measured by Researcher 1.

Table 9 shows that for 3 (2.9 %) of the 102 sample images scored, only 1% of the population was closer to the sample than the target; 16 (15.7%) of the samples found their target within 5% of the population; and 23 (22.5 %) of the samples found their target within 10% of the population.

Edited 10/11/13

Figures 34 and 35 provide different views of the performance of the Distance Metric Model. Figure 34 shows a distance Cumulative Density Function for each sample. That is, each sample has a curve showing how fast the percent of the population increases with distance measured from that sample. Curves toward the left of Figure 35 correspond to Samples for which there are nearby members of the population, while curves toward the left correspond to samples for which there are very few nearby members of the population. Curves that rise sharply are including regions in which the population is dense, so a slight increase in distance includes many additional members of the population. On the other hand, curves that rise slowly are including regions in which the population is sparse, so even a relatively large increase in distance includes few additional members of the population.

In Figure 34, the blue circles represent the Target for each sample; a blue circle near the horizontal axis represents a target close to its sample, while a blue circle in the upper half of the figure represents a target far from its sample.

Figure 35 is a Cumulative Density Function, a graphical representation of the information in Table 8. It plots the percent of the Population closer to each Sample than its corresponding Target. There are 23 Samples whose Target is within 10% of the Population and 49 Samples whose Target is within 40% of the Population. Of course, the worst case Sample finds its Target within 100% of the Population. If the Distance Metric Model is performing well, the graph remains low through many Samples, jumping up to 100% only for the few Samples it finds far from their respective Targets.

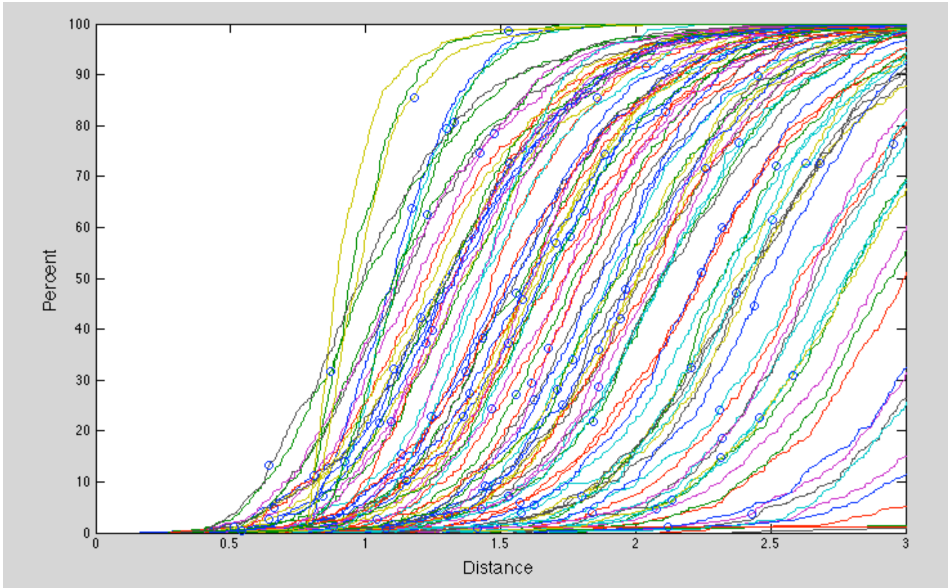

Figure 34. Proportion of Population vs. distance for each upper jaw Sample scored by researcher 1.

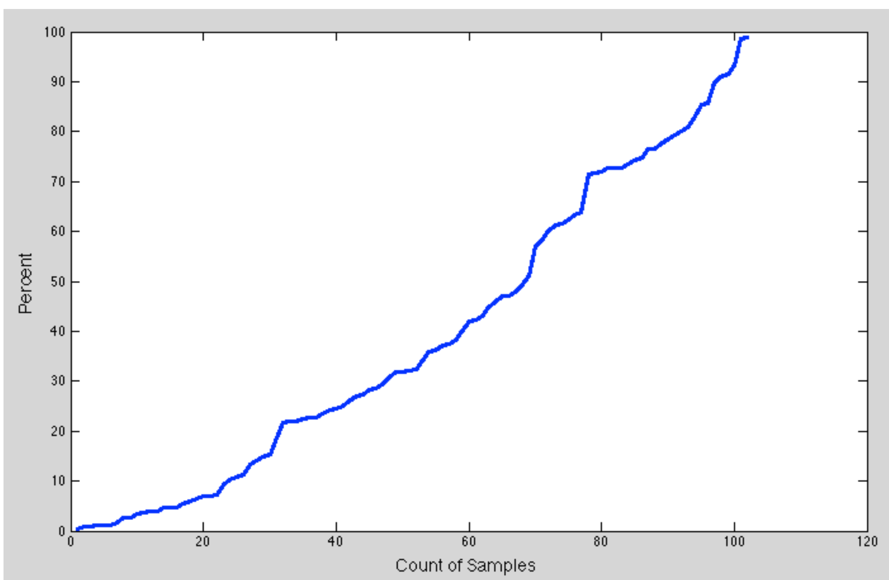

Figure 35. Cumulative Density Function, a graphical representation of the information in Table 8, the percent of the Population closer to each Sample than its corresponding Target.

In principle, the distance can be computed using any subset of the 10 factors provided in the data set. For example, if we ignore the tooth width measurements and use only the factors representing measurements of angles, we get the results shown in Table 9.

```
           Average target percent: 26.2
               Sample count:    95
Within  1% of population:   8,  8.4 % of samples
Within  5% of population:  24, 25.3 % of samples
Within 10% of population:  35, 36.8 % of samples
```

Table 9. The Percent of Population closer to selected Sample than the corresponding Target for upper jaw Samples measured by researcher 1, using use only the factors representing measurements of angles.

Compared with Table 8, Table 9 shows that omitting tooth width factors improved the overall performance from an average target percent of 39% to 26%, and 8%, 25%, and 37% (vs. 3 %, 16 %, and 22 %) of the Samples found their corresponding Target within 1%, 5%, and 10% of the Population, respectively. The Sample count decreases because the number of Samples with a relatively high proportion of missing information increases.

Figure 36 corresponds to Figure 34, except that the Distance Metric Model is using use only the factors representing measurements of angles. The red, magenta, and green curves are the density functions for the samples. If the magenta curve is toward the left of the figure, it indicates that the sample is in a region where the population is dense, yielding 23% of the population closer than the corresponding target, while the red curve is toward the right of the figure, indicating that the sample is in a relatively sparse region of the population, yielding only 4.8 % of the population closer than the corresponding target.

Figure 37 shows the Cumulative Density Function corresponding to Figure 36, except that the Distance Metric Model is using use only the factors representing measurements of angles. The blue curve for the smaller six-factor model remains low for more samples, indicating its improved performance.

Edited 10/11/13

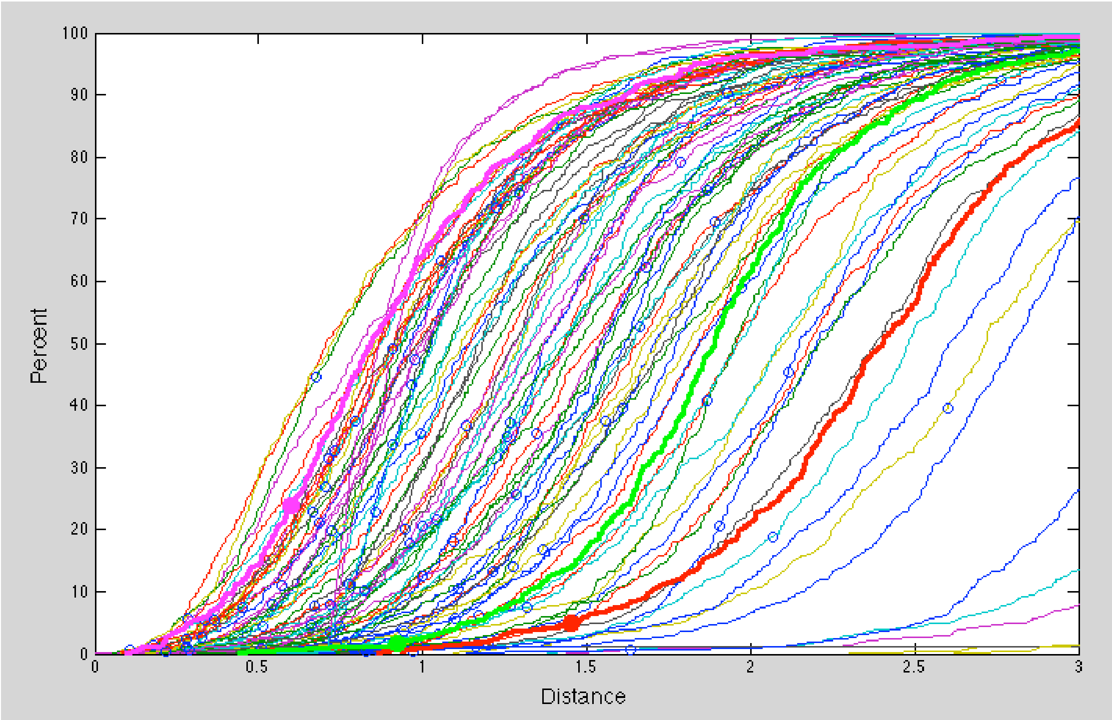

Figure 36. Proportion of Population vs. distance for each upper jaw Sample scored by researcher 1, using use only the factors representing measurements of angles.

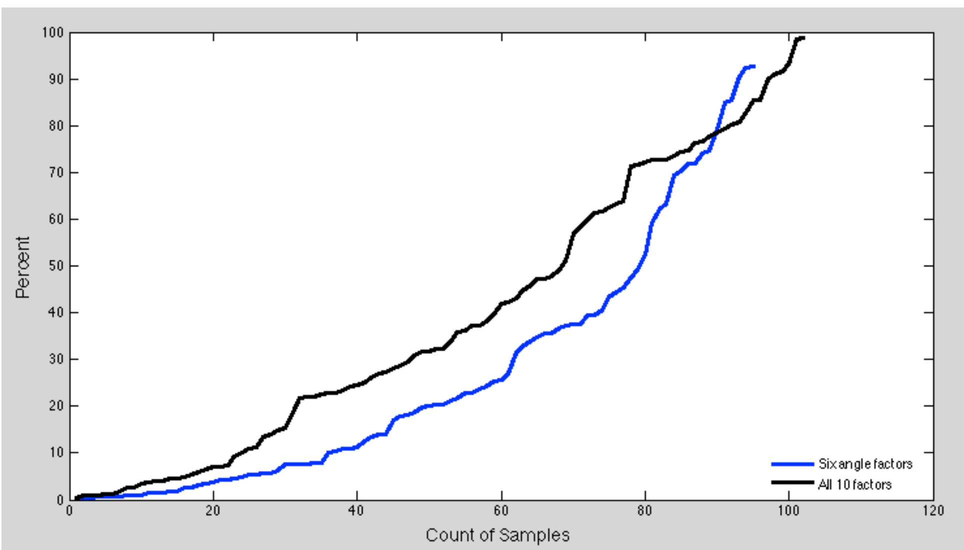

Figure 37. Cumulative Density Function, showings the percent of the Population closer to each Sample than its corresponding Target.

Edited 10/11/13

This presents only the results from upper jaw Samples and Populations measured by Researcher 1 to help explain the Distance Metric Model. Table 9 shows the percent of population closer to selected sample than the corresponding target, using only the factors representing measurements of angles, for both lower and upper jaws and for the measurements from both researcher 1 and researcher 2. For this data set, the Distance Metric Model performs a little better on the upper jaw samples than on the lower jaw samples, and there was no appreciable difference in performance using the sample and population measurements of each researcher.

In comparing the results in Table 9 with those in Table 10, the Distance Metric Model seemed to perform better ignoring the tooth width factors and using only the angle factors. Table 11 summarizes the performance of the Distance Metric Model using several different factor subsets:

- All ten factors, four tooth width factors and six angle factors,
- Six angle factors,
- Five angle factors, omitting the first of the six (angle AB),
- Five angle factors, omitting the second of the six (angle AC),
- Five angle factors, omitting the third of the six (angle AD),
- Five angle factors, omitting the fourth of the six (angle BC),
- Five angle factors, omitting the fifth of the six (angle BD), and
- Five angle factors, omitting the sixth of the six (angle CD).

Lower - Investigator 1		
Count samples:	125	
Samples within	1 % of the population	6 4.8 % of the samples
Samples within	5% of the population	25 20.0 % of the samples
Samples within	10 % of the populatio	36 28.8 % of the samples
Lower - Investigator 2		
Count samples	132	
Samples within	1 % of the population	5 3.8 % of the samples
Samples within	5% of the population	23 17.4 % of the samples
Samples within	10 % of the populatio	33 25.0 % of the samples
Upper - Investigator 1		
Count samples	95	
Samples within	1 % of the population	8 8.4 % of the samples
Samples within	5% of the population	24 25.3 % of the samples
Samples within	10 % of the populatio	35 36.8 % of the samples
Upper - Investigator 2		
Count samples	98	
Samples within	1 % of the population	9 9.2 % of the samples
Samples within	5% of the population	26 26.5 % of the samples
Samples within	10 % of the populatio	32 32.7% of the samples

Table10. Illustration of the percentage of Population closer to selected Sample, than the corresponding Target, use only the factors representing measurements of angles.

Each row in Table 11 summarizes performance as shown in the "In total:" portion of Table 3 for each subset of factors, across both lower and upper jaws and across both researchers For this data set, the Distance Metric Model using only the six angle factors performed better than when also using the four tooth width factors. No further improvement was observed by omitting any one of the six angle factors.

Factors	Population count within 1% (%)	Population count within 5% (%)	Population count within 10% (%)	Samples
All 10	14 (2.9)	69 (14.1)	117 (23.9)	489
Six angles	28 (6.2)	98 (21.8)	136 (30.2)	450
Omit 1st of 6	32 (7.5)	93 (21.7)	142 (33.1)	429
Omit 2nd of 6	29 (6.8)	97 (22.7)	138 (32.3)	427
Omit 3rd of 6	28 (6.4)	92 (20.9)	140 (31.8)	440
Omit 4th of 6	26 (6.2)	85 (20.4)	130 (31.2)	417
Omit 5th of 6	26 (6.0)	95 (22.1)	130 (30.2)	430
Omit 6th of 6	25 (5.8)	78 (18.2)	126 (29.4)	428

Table 11. Total performance using different factor subsets in the Distance Metric Model.

In summary, in more than 20% of the Samples in this study, the Distance Metric Model finds the Target within the closest 5% of the Population. In more than 6% of the Samples, it finds the Target within the closest 1% of the Population. This demonstrates that it is often possible to determine scientifically that a given Sample must belong to a very small (e.g., 5% or even 1%) proportion of the Population.

Results of forces applied

Using the SAS® System and incorporating the Means Procedure, the Phidgets log record for bite infliction recorded 4684 points of data during the course of the production and documentation of 200 patterns on twenty-five pigs. The mean recording for all points in which pressure was applied with the replication device was 545.62with a standard deviation of 278.78 within the range of pressures recorded for each event between 0 and 997.00on the FlexiForce® to the computer with a Phidgets device. Each of the Flexi Force® sensors was bridged to the computer with a Phidgets device. Each of

Edited 10/11/13

the sensors had been bench calibrated with an Omega model LCKD-100 load cell. Force versus Time was plotted for each pig location. As an example, Pig 25 L A (left side, position A) is represented in figure 38 and the resultant bite pattern can be seen in figure 39. Each of the 200 patterns was similarly correlated to the maximum force of the device over a period of 15 seconds.

Image measurement using Tom's Toolbox© began, once the 200 highest quality images were selected and their resolution established at 300 dpi and their file format as TIFF verified. Of particular importance were the images and resultant forces producing them that lead to a high degree of inter-operator agreement. Pig 19R using blind model 659 was directly correlated to the stereolithography model from the original series represented by model number 945. The resultant pixel placement and forces used to create the bite mark are illustrated in Figure 40.

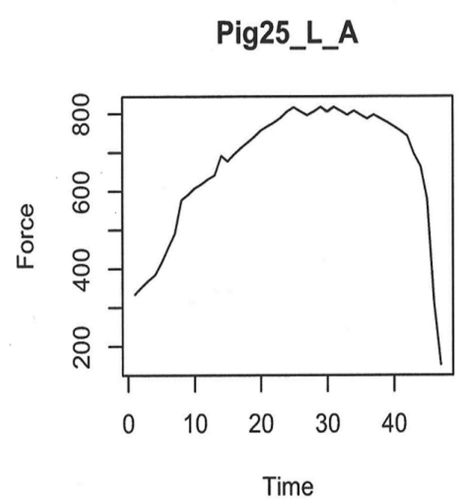

Figure 38. Analysis variable for pig number 25 left side site A, or hind limb, representing the mean force of 665.553191 Phidgets sensor reading with minimum and maximum loads over 20 second maximum load force.

Figure 39. Illustrates a replicated bite mark with a mean force of 665.553191 Phidgets sensor reading. start_side_site=Pig19_R_A.

Conclusions

Discussion of Findings

Many factors exist which can alter the value and weight that should be given to the Interpretation of a patterned injury. These include, but are not limited to, the applied force, the area of the body where the bite occurred (e.g., the skin on the human back is much thicker, as opposed to that of the female breast) Rawson [27], the underlying structures beneath the skin, whether the bite occurs ante mortem, peri mortem, or post mortem and the techniques used in the preservation and analysis. Any of these may affect the ability of the examiner to be able to correlate the patterned injury with any degree of scientific probability to a known individual.[28] [29] [30] [31] In one study, 50 volunteers were selected to inflict bite marks on each other, the patterns were analyzed by two photographic techniques that included painting and a 2D Polyline technique, measuring the arch width from cusp tip to cusp tip and the angle of rotation from this base-line along the mesial distal widths of the incisal edges of the four anterior teeth.[32] Measurements were made using the tools found in Adobe Photoshop, which required hand-eye coordination. Additionally, measurements in Adobe Photoshop are limited by the software to the nearest tenth of a decimal point. The authors' previous studies provided a methodology to standardize measurements and accuracies in both the two-dimensional and three- dimensional planes. [2] [10] Inter-operator and intra-operator error rates have been reported. Forces and stresses necessary to inflict a bite mark patterned injury have been limited to either individual pig models [16] or the use of limited number of human cadavers. [19] For a number of reasons, statistical comparisons of results from these previous studies were not possible. There was no method of comparing results to a known data set, reflecting a specific population group. In a study by Bush , a single model was physically changed by grinding away the incisal edges of existing teeth to show substantive changes in reported angles of rotation regardless of how these nine changes would have occurred, or if they were present in a given population.[30] These changes would not have involved physiologic changes such as mesial drift of the teeth that occurs with the forces of mastication nor the loading and tilting of dentitions that naturally occur when inflicting a patterned injury in vital skin. A cadaver model has its own sets of limitations such as the inelasticity of the skin, the lack of an inflammatory response that enhances patterns in vivo and the ability of tissue to maintain the patterns, when the event is coordinated with a peri-mortem period. Porcine skin has been shown to offer the best experimental model for research as a substitute for vital human skin. [18] Other investigators have noted that the dermal-epidermal ratio in the porcine model is comparable to those of human skin [33], and that the kinetics of epidermal proliferation, cell layering and the elastin deposits are remarkably similar to humans. A search of current literature did not find a study that correlates quantified human dental characteristics in a known data set to an individual bite mark pattern.

The 2009 National Academy of Science report, *Strengthening Forensic Science in the United States: A Path Forward*, has energized the field of Forensic Odontology to search for more scientific methods eliminating subjectivity, bias, and the misinterpretation of results. [1] In fact, since 1984 and long prior to the NAS 2009 recommendations, the American Board of Forensic Odontology (ABFO), has been developing guidelines. The National Academy of Science Report states that more scientific methods should be initiated in all of the comparative sciences. [1] To accomplish this objective, a series of studies was instituted to establish a methodology for constructing a dataset of dental characteristics, quantify dental characteristics in both two dimensional and three dimensional views and establishing reliability of measurements in both intra and inter operator error analysis. The initial quantifications of widths, damages, angles of rotation, missing teeth, diastema and arch width analysis, were subsequently augmented by displacement and three dimensional analyses. [2] [3] [5] [10] This study adds practical application of these data sets to replication of patterned injury in porcine skin and the interpretation of the combination of quantified characteristics of the dental arches making up the initial data set. Additionally information regarding intersecting angles formed by extending incisal lines to adjacent and cross arch teeth accounted for the ability to accurately access rotations when the native curve could not be generated. In doing so, the criticisms of past investigators regarding bias, distortion, replication and interpretations were addressed. Ball introduced the basis for errors in utilizing an acetate overlay technique in bite mark pattern analysis in which a sheet of acetate paper is used to trace the biting edges of and then comparing those visually to a patterned injury.[34] Errors in digital photography, the lack of standardized methodology, subjectivity in generating overlays, problems with accuracy and problems with reproducibility along with photographic distortions, and the reliability of computer generated overlays were among the most significant criticisms. Ball concludes that a standard was not established by this method alone. [34]

The initial portion of this study focused on creating a bite pattern in porcine skin that could be quantified. In order to accomplish this goal, a method of delivering a force that could provide a distinct pattern in skin was developed. There have been numerous studies that have reported bite forces in the anterior tooth region that range from 20-22 PSI to 122 PSI. [15] [35] [36] [37]. The forces are influenced by numerous factors. Koc et al described these influential factors as pain, gender, age morphology and the individuals existing occlusion pattern. [38] Our determination of bite force needed to create a patterned injury was based on our findings of a range between 25 and 131.1 PSI was consistent with these reports. Calibrating each device and measuring forces inflicted during the biting process added consistency and repeatability to the process of creating a bite that would closely replicate an actual event. As Koc, et.al. concluded: "….recording devices and techniques are important factors in bite force measurement Therefore, one should be careful when comparing the bite force values reported in the research." [38] The use of a Flexiforce® transducer (FlexiForce®, Tekscan Inc., South Boston, USA) has been previously reported. [21] Because the scale established thru the Phidgets device did not report in pounds per square inch, the FlexiForce® sensor imbedded in each set of the 50 pattern replication devices required calibration prior to each pig session. This insured that forces applied were within the physiologic range and consistently applied.

Porcine skin has been established as an in vivo model for human skin. [17] A number of citations in the literature point to distortions common to patterned injury evaluation in skin. [39] [40] Sheasby and MacDonald reported on a classification system. [39] They concluded that distortion can occur at various stages during the biting process. If it occurs at "the time of biting" they defined this as "primary distortion." [39] If distortion occurs subsequent to the biting, this was defined as "secondary distortion." Sheasby and MacDonald further point out that primary distortion can occur either as a dynamic or as a tissue component. Distortion is produced by the dynamics of biting and depends on the degree of movement during the process. If movement is absent or slight a static bite mark may result. With extreme movement the bite mark appears distorted and linear striations (scrape marks) may be present. Additionally they point out that the quantity of tissue is taken into the mouth may produce "tenting" of the tissue which results in dimensional changes in the skin. They also classify three categories of secondary distortion. These would be distortions that are time related, posture distortion and photographic distortion. .An exact match in arch size is fortuitous and unpredictable. Exact superimposition is only possible in bite marks exhibiting minimal distortion and size matching techniques are only applicable to bite marks exhibiting minimal distortion. The incidences of discrete morphological points of comparison or distinctive features in a bite mark are the most significant criteria in bite mark analysis since they are relatively immune to distortion. As the degree of distortion increases, bite mark analysis relies progressively more on distinctive features [39]. This project aimed at producing as little distortion as possible. Pigs 1, 2 and 3 demonstrated the distortion and lack of pattern production in a dynamic bite (see Figure 41) further evidence that, underlying tissue morphology can also impact bite mark interpretation. [27]

Figure 40. An illustration of the lack of a distinct pattern in a dynamic bite.

Kieser et al, characterized the uniqueness of the human anterior dentition. [41] The authors found uniqueness of the anterior dentition in both arches based on geometric morphometric analysis of individuals that were selected because they had similar orthodontic treatment, making their dentitions similar at the onset of the investigation. The geometric morphometric analysis focused on capturing subtle differences about morphology and spatial locations of the anterior teeth in both arches The study supported the findings of Rawson's initial study which concluded that certain characteristics occur that are inter related. These include, shape, number, mesio-palatal rotations and restorations. [42] These results were substantiated by our initial investigations. [2][3][5][10]. Not used in prior investigations was the concept of measuring angles formed by the intersecting extension of a line drawn on the incisal edge of each of the 4 anterior teeth in each arch. These were computed by placing markers directly opposite of each other on the mesial and distal outline of the teeth in a recognizable patterned injury. The principle of intersecting angles being that parallel lines do not cross and line segments continue past the incisal widths to intersect in a two dimensional photograph regardless of curvatures in the skin. Thus the concept of intersecting line angles is based on this incisal line, which the authors define as a straight line across the incisal edge of the teeth connecting the mesial to the distal most point on the tooth's biting (incisal) edge. This line intersects with adjacent incisal lines of the other anterior teeth at a measurable angle and is graphically represented in figures 41.

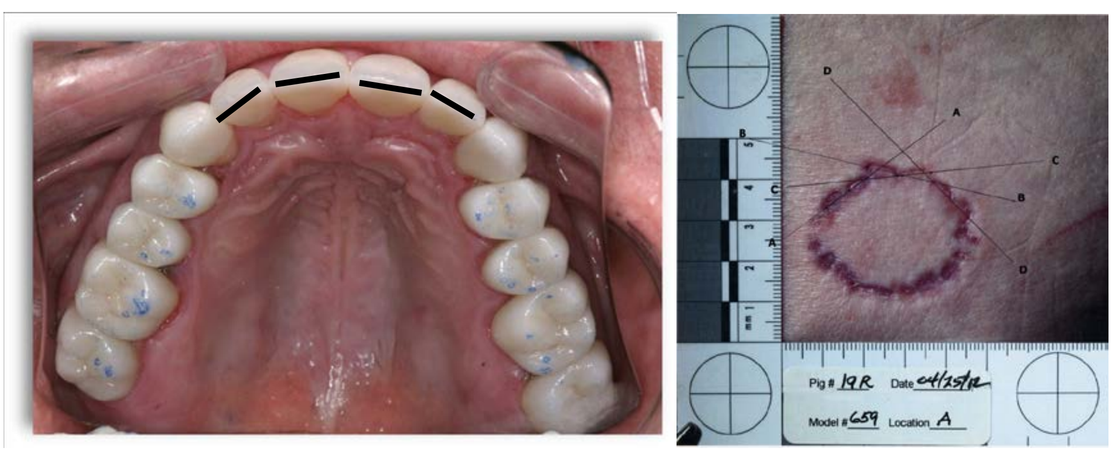

Edited 10/11/13

Figure 41. Extension of the incisal lines of the anterior teeth eventually intersect with an adjacent incisal line, forming a measureable angle. The angles of intersection for the maxilla are illustrated in this image. Intersecting incisal lines forming angles AB, AC, AD, BC, BD and CD in the four maxillary incisors. Tooth 10=A, Tooth 9=B, Tooth 8=C Tooth 7=D.C (Actual photo on right is a scaled view of figure 28 for comparison)

Reliability enters into any discussion of the comparative sciences. A number of authored opinions are critical of such issues as the direct comparison methods [43], the lack of reporting of error rates [44], the claims of uniqueness [45] and the reliability of testing. [46]. In addition, photographic techniques have been questioned. The American Board of Forensic Odontology has established among their guidelines one that address distortions in photography. [48] These and SWIGIT guidelines were rigorously followed in the documenting of the photographic images used in this study. Within this study were the inter operator error rates established for the known group of data. As reported by using two methods of statistical analysis inter-operator agreement was 0.984 in the known population, using Pearson correlation and within 1% of each other when calculating the population closest to the target using distance metric analysis. Because the individual characteristics of the human dentition do not transfer equally, the authors recommend using all the characteristics previously cited in the literature in analyzing a patterned injury. The substrate in which the pattern occurs will dictate the weight given to each characteristic. In this study, widths were not transferred from the natural dentition to the porcine skin as readily as the characteristics of intersecting angles. For porcine skin, the characteristics of intersecting angulation, displacement, individual missing teeth, rotations, spacing or diastemas and angulation of teeth to the x/y axis if posterior teeth are in the pattern, visually appear to transfer well and need further

Edited 10/11/13

analysis . Tom’s Toolbox has proven to be a valuable asset in quantifying individual patterns. The authors suggest that for the imaging specialist it can serve as asset in initial evaluation of bite patterned injuries.

Implications for policy and practice.

Interest in the forensic value of patterns caused by human teeth (bite marks or tooth marks) has a long history. Anecdotal history records Agrippa recognizing the decapitated head of a rival from a peculiar tooth. Early in legal history, tooth patterns were used to authenticate a document by having the responsible official bite into the sealing wax when it was applied to the document. The literature later records the use of dental charts and radiographs in human identification. The value of patterns produced by teeth (bite marks) have long been considered by many scientists world-wide, as possible identifiers of the individual. It is assumed by most dentists, that the characteristics of the human dentition are unique to each individual. Evidence in the research literature supports this concept. [42],[43],[44],[45],[46] Disagreements exist between scientists occur over whether these unique patterns of the human dentition, if true, can be replicated in human skin. Although human tooth patterns can and have occurred in inanimate objects, those that that are present in human skin, because of its viscoelasticity, present the most difficulties in interpretation. Several variables can and do occur. Distortions, either dynamic or photographic are the most common problems. The ABFO Standard Reference Scale #2 with its three circles, was developed by George Hyzer and Thomas Krauss and provided a means of detecting and correcting moderate photographic distortion. It is broadly accepted in evidence photography [47]

The production of a legible pattern replicating the pattern of teeth in skin depends upon multiple factors in addition to the substrate and the mechanism. Firm substrates such as cheese, soap, plastic and leather, to cite several media, register dimensions best. The mechanism can be divided into two categories; dynamic and static. Dynamic distortion occurs when there is movement by either or both victim and assailant. Static distortion occurs less commonly and in the opinion of the authors occurs more often in the pattern of the lower teeth since the mandible is not fixed in position, as is the maxilla. Another variable, even in a static bite is the degree of elasticity in the skin and the inability to capture the exact dimensions of the teeth. The evidentiary value of the injury pattern can be influenced by the amount of distortion in the injury pattern. Even when agreement exists in the analysis of a pattern between all examiners, there is still a need for a scientific level of confidence for the opinion. This research is only a template for continued research. It is not the Rosetta stone. Continued research to develop this relatively new applied science of pattern analysis should not be stifled. The National Academy of Science Forensic Report in 2009, *Strengthening Forensic Science in the United States: A Path Forward*, recommended that scientific methods be initiated in all of the comparative sciences. [1]

Whether dental characteristics are reliably replicated in a bite mark in human skin and whether the replicated pattern can be correlated with a degree of probability to the source is the current challenge. Several recently published studies have demonstrated that at least seven characteristics of the human dentition can be quantified. [2] [5] [10] A data set quantifying eight dental characteristics, in both two and three-dimensions, has now been developed from research and published by the authors.

Edited 10/11/13

The scientific validation of the correlation of bite marks, or tooth patterns to their origin, in the opinion of the authors, predictably will be established by statistical / mathematical probability. That is, which combination of outlying characteristics demonstrated in a pattern(s) would reliably predict the probability of another individual in the population having the same combination of dental characteristics? For those images of the patterned images that include all six anterior teeth, or even several teeth that enable the investigators to insert markers, measurements were saved in Tom's Toolbox©, calculated, saved in an internal data set and an internal report function ranks the combination of characteristics in percentiles. The application also established outliers for those specific characteristics.

Prior to this report, to accomplish the frequency distribution of the dental characteristics, which make each individual's dentition individual, a series of studies were instituted to establish a methodology for quantification in both two and three-dimensions. This methodology was utilized to build a dataset of seven dental characteristics. Additional research established the reliability of the measurements, testing both intra-operator and inter-operator agreement in analysis. The initial quantification of width, damage, angles of rotation, missing teeth, diastema characteristics (spaces) and arch length were subsequently augmented by a study of displacement of the anterior teeth, either labially or lingually, from the normal physiologic dental arch form. A three- dimensional study of the width and incisal position of the anterior teeth on the horizontal (Z) plane supplemented the data. This study adds a practical application of the data set. An additional geometric approach to determining the angles of rotation of the four maxillary and mandibular incisors was developed. This concept utilizes the measurement of the angels at the intersection of the incisal lines, projected through the mesial and distal markers of each of the incisors. This geometric method of determining rotation through the measurement of the intersecting angles of the incisal lines is beneficial for several reasons. First, it eliminates subjective establishment of a base X axis. It is also more universal. One or more teeth may be missing or indistinct. If two or more anterior teeth can be identified (e.g. tooth 7 and 9), computation of the angle of intersecting lines can still be determined. This method of establishing tooth rotation also provides an expanded scope of search analysis, since it includes two additional characteristic items. In the earlier studies when an x axis could be established, we were able to determine four angles of rotation. With the alternate method of utilizing the intersecting angles formed by the incisal lines, enable the measurement of six angles of rotation.

Although the width of the teeth in injury pattern in skin may be less exact than that of the known source, the intersecting angle formed by the extension of the incisal lines remains a constant. Most significant in establishing the degree of probability of a correlation will be the presence of multiple outliers in these angles. This procedure adds four additional characteristics to enable statistically the probability of a correlation between the unknown and a known source.

The interpretation of the combination of quantified dental characteristics making up the initial two-dimension data set, also utilized the data obtained in the three-dimensional study, since the anterior teeth are not always all at the same level of eruption (Z plane). In doing so, the questions regarding whether certain teeth were present or missing in a patterned injury cited by past investigators were addressed.

In more than 20% of the Samples in this study, the Distance Metric Model found the Target within the closest 5% of the sample population. In more than 6% of the Samples, it found the Target within the closest 1% of the Population.

Implications for further research

This study demonstrates that it is sometimes possible to replicate patterns of human teeth in porcine skin and determine scientifically, that a given injury pattern (bite mark) belongs to a very small proportion of our population data set, e.g. 5%, or even 1%. Predictably, building on this template, with a sufficiently large database of samples reflecting the diverse world population, a sophisticated imaging software application requiring operators inserting parameters for measurement and additional methods of applying forces for research need further investigation. This is applied science for injury pattern analysis and is only foundational research. It should not be cited in testimony and judicial procedures. It is intended to supplement and not contradict current guidelines of the American Board of Forensic Odontology (ABFO) concerning bite mark analysis and comparisons. A much larger population data base must still be developed. This research serves as a template, refining the ability to scientifically calculate that an unknown bite mark replicated in skin can correlated with probability to a member of the population data base. This template does not limit future researchers to use specific imaging software or pattern replication apparatus. All of the research materials and records will be maintained by Marquette University for a period of three years for repeatability of the study. The authors encourage questions and challenges.

1. Marquette University School of Dentistry; 2. Medical College of Wisconsin; 3.Marquette University College of Engineering; 4.Wisconsin Department of Justice, Crime laboratory, (retired).

References

1. The National Academies Press web pages. http://books.nap.edu/openbook.php?record_id=125898page=85; last accessed June 1, 2013.

2. Johnson LT, Radmer TW, Wirtz TS, Pajewski NM, Cadle DE, Brozek J, Blink DD; Quantification of the Individual Characteristics of the Human Dentition J For Ident, Vol 59 (6), November/December 2009 pp 607-623.

3. Radmer TW, Johnson LT; the Correlation of Dental Arch Width and Ethnicity, J. For Ident, Vol. 59 (3) May/June 2009 pp 268-274.

4. Johnson LT, Blinka DD, VanScotter-Asbach P, Radmer TW; Quantification of the Individual Characteristics of the Human Dentition: Methodology, J For Ident, Vol. 58 (4) July/August 2008, p 409-418.

5. Radmer T, Johnson LT; the Quantification of Tooth Displacement, J For Ident, Vol. 60 (3) Mar/Apr 20106.

6. Moreira C et.al; Assessment of Linear and Angular Measurements on Three Dimensional Cone-beam Computed Tomographic Images, J Oral Surg Oral Med O, 2009, September 108(3), 430-436.

7. Lopes PML, et.al; 3-D Volume Rendering Maxillofacial Analysis of Angular Measurements by Multislice CT, J Oral Surg Oral Med O., 2008, February; Vol 105(2), 224-230

8. Brown AA, Scarfe WC, Scheetz JP, Silveira AM, Farman AG; Linear Accuracy of Cone Beam CT Derived 3D Images, The Angle Orthodontist, 2009 January, Vol 79(1) 150-157.

9. Rahimi A, et al; 3-D Reconstruction of Dental Specimens from 2D Histological Images and µCT-Scans, Comp Meth Biomech Biomed Eng, 2005, June Vol 8 (3), 167-176.

Edited 10/11/13

10. Johnson LT, Radmer TW, Visotcky AD, Ahn KW, Blinka DD; A Methodology for Three-Dimensional Quantification of Anterior Tooth Width, J For Ident, Volume 61, No. 3, (2011), pp. 296-310.

11. MacFarlane TW, MacDonald DG, Sutherland DA; Statistical Problems in Dental Identification, J For Sci Soc, 1974, 14(3), 247-252.

12. Rawson RD, Ommen RK, Kinnard G, Johnson J, Yfantis A; Statistical Evidence for the Individuality of the Human Dentition, J For Sci 1984, 29(1), 245-253

13. Barsley RJ, Lancaster DM; Measurement of Arch Widths in a Human Population: Relation of Anticipated Bite Marks, J For Sci. 1987, 32(4), 975-982.

14. Bernitz H, vanHeerden WF, Solheim T, Owen JH; A Technique to Capture, Analyze and Quantify Anterior Teeth Rotations for Application in Court Cases, J For Sci 2006, 51(3), 621-629.

15. Anusavice, K J., Phillips, RW; Science of Dental Materials, 11th edition. 2003, Chapter 4, Mechanical Properties of Dental Materials, p 93, Saunders, Philadelphia, Pennsylvania, USA.

16. Avon SL, Mayhall JT, Wood RE; Clinical and Histopathological Examination of Experimental Bite Marks In-vivo. J Forensic Odontostomatol, 2006, Dec; 24(2): 53-62.

17. Avon S. L., Wood RE; Porcine Skin as an In-vivo Model for Ageing of Human Bite Marks; Journal of Forensic Odonto-Stomatology, 2005 December Vol 23(2): 30-39.

18. Valdaxis NJ, Brans TA, Boon ME, Kreis RW, Marres LM; Confocal Laser Scanning Microscopy of Porcine Skin: Implications for Human Wound Healing Studies, J Anat, 1997; 190, 601-611.

19. Bush MA, Thorsrud K, Miller RG, Dorion RBJ, Bush PJ; the Response of Skin to an Applied Stress: investigation of Bite Mark Distortion in a Cadaver Model, J For Sci, 2010, Jan; 55 (1): 71-76.

20. Flexforce™http://www.trosenrobotics.com/flexiforce-1lb-resistive-forcesensor. aspx>feed=Froogle (Last visited 06/12/2013).

21. Bousdras VA, Cunningham JL, Ferguson-Pell M, Bamber MA, Sindet-Pedersen S, Blunn G, Goodship AE; A Novel Approach to Bite Force Measurements in a Porcine Model In Vivo, Int J Oral and Maxillofac Surg 2006, 35: 663-667.

22. Valdaxis NJ, Brans TA, Boon ME, Kreis RW, Marres LM; Confocal Laser Scanning Microscopy of Porcine Skin: Implications for Human Wound Healing Studies. J Anat 1997; 190, 601-611.

23. Avon SL, Mayhall JT, Wood RE; Clinical and Histopathological Examination of Experimental Bite Marks In-vivo. J Forensic Odontostomatol 2006, Dec; 24(2): 53-62.

24. Koc D, Dogan A, Bak B; Bite Force and Influential Factors on Bite Force Measurement: a Literature Review, Eur J Dent 2010 Apr 4(2) 223-232.

25. American Board of Forensic Odontology, Diplomate Reference Manual, January 2013 Edition, pp1-17.

26. American Board of Forensic Odontology, Diplomate Reference Manual, ww.abfo.org last accessed 06/12/2013.

27. Rawson RD, Brooks S; Classification of Human Breast Morphology Important to Bite Mark Investigation, Am J of Forensic Medicine and Pathology, March 1984, vol 5 Number 1, pp19-24.

28. Bernitz H, Owen JH, van Heerden WF, Solheim; An Integrated Technique for the Analysis of Skin Bite Marks. J For Sci, 2008, Jan; 53(1): 194-8.

29. Pretty IA; the Barriers to Achieving an Evidence Base for Bite Mark Analysis. Forensic Sci Int, 2006 May 15; 159 Suppl 1:S110-20 Epub 2006 Mar 15.

30. Bush MA, Miller RG, Bush PJ, Dorion RB; Biomechanical Factors in Human Dermal Bite marks in a Cadaver Model. J For Sci, 2009 Jan, 54(1): 167-76.

31. Metcalf RD; Yet Another Method of Marking Incisal Edges of Teeth for Bitemark Analysis. J For Sci, 2008, Mar; 53(2): 426-9.

32. Al-Tlabani N, Al-Moussawy ND, Baker FA, Mohammed HA; Digital Analysis of Experimental Human Bitemarks Application of Two New Methods. J For Sci, 2006, Nov; 51(6): 1372-5.

33. Rose EH, Kasander GA, Vistnes LM; A Micro Architectural Model of Regional Variations in Hypodermal Mobility in Porcine and Human Skin. Annals of Plastic Surgery, May 1978 vol 1 (3), 252-266.

34. Ball J; A Critique of Digital Bite mark Analysis, Thesis Centre for Forensic Science, University of Western Australia, 2004, pp10-139.

35. Raadsheer M C, vanEijden T, vanGinkel F C, Prahl-Andersen B; Contribution of Jaw Muscle Size and Craniofacial Morphology to Human as Bite Force Magnitude, J Dent Res, 78(1) January 1999, 31-42.

36. Pandula V; http://www.junior dentist.com/ what-are-masticatory-forced.html. Last visited Oct 30, 2012.

37. Demirhan D, Burak G, Kerem A, Ayse K, Cihan A; Maximal Bite Force Measurement By The “ Istanbul Bite Force Recorder”, FTR Bil Der J PMR Sci 2008; 3:117-123.

38. Koc D, Dogan A, Bek B; Bite Force and Influential Factors on Bite Force Measurements: A Literature Review, Eur J Dent 2010 April: 4(2): 223-232.

39. Sheasby DR, MacDonald DG; A forensic classification of distortion in human bite marks, For Sci International 122 (2001) 75-78.

40. Millington P; Histological Studies of Skin Carrying Bite Marks, J For Sci Soc 1974, vol 14(3)239-40.

Edited 10/11/13

41. Kieser JA, Bernal V, Waddell JN, Raju S; The Uniqueness of the Human Anterior Dentition: Geometric Morphometric Analysis, J Forensic Sciences, May 2007, Vol 52, Issue 3 pp671-677

42. Rawson RD, Ommen RK, Kinard G, Johnson J, Yfantis A; Statistical evidence for the individuality of the human dentition, J Forensic Sci 1984; 43; p245-53.

43. Bowers M; Problem based analysis of bite mark misidentifications. What DNA has done to contradict opinions of odontologists trained before the New Millennium, For Sci Int 2006 May 15; Suppl 1, S104-109.

44. Kostelnik K, Cohrn K, Byrd J; Freeing the Innocent: When Guilty Convictions are Overturned due to errors in Bite Mark Analysis , University of Florida honors program web site www.honors.ufl.edu/apps/Thesis.aspx/Details/1694 last accessed 03/07/2013

45. Cole S; Forensics without uniqueness, conclusions without individualization: the new epistemology of forensic identification, Law, Probability & Risk, Sep 2009, vol 8 Issue 3 p233-255

46. Page M, Taylor J, Blenkin M; Uniqueness in the forensic identification sciences- Fact or fiction? , Forensic Science International, March 2011, vol 206 Issue 1-3, p12-18.

47. Hyzer G, Krauss T; ABFO Standard Reference Scale #2; J Forensic Sci 1988 Mar 33(2): 498-506.

Dissemination of Research Findings

1. A one hour summary of the research was presented to the Marquette University School of Dentistry faculty and students, July 16, 2013, Milwaukee Wisconsin.
2. A one hour summary of the research was presented to the graduate students and faculty in the Department of Biomedical Engineering, Marquette University, College of Engineering on November 12, 2012.

3. A one hour PowerPoint summary of the research findings was presented at the 97th Annual Educational Conference of the International Association for Identification, on August 5, 2013 at Providence, Rhode Island.
4. A lecture capture video of the research has been recorded for dissemination via a link posted on several forensic organizations' web pages is being prepared for distribution. The Midwest Forensic Resource Center and other forensic organizations have been approached requesting that they post a link to the video on their web sites.
5. Overtures have been made to the National Association of Medical Examiners (NAME) and regional / state divisions of the International Association for Identification as possible educational presentations.

Edited 10/11/13